

1961

The crystal structure of bismuth monochloride

Alexander Hershaft
Iowa State University

Follow this and additional works at: <https://lib.dr.iastate.edu/rtd>

 Part of the [Physical Chemistry Commons](#)

Recommended Citation

Hershaft, Alexander, "The crystal structure of bismuth monochloride " (1961). *Retrospective Theses and Dissertations*. 2435.
<https://lib.dr.iastate.edu/rtd/2435>

This Dissertation is brought to you for free and open access by the Iowa State University Capstones, Theses and Dissertations at Iowa State University Digital Repository. It has been accepted for inclusion in Retrospective Theses and Dissertations by an authorized administrator of Iowa State University Digital Repository. For more information, please contact digirep@iastate.edu.

This dissertation has been 61-3037
microfilmed exactly as received

HERSHAFT, Alexander, 1934-
THE CRYSTAL STRUCTURE OF BISMUTH
MONOCHLORIDE.

Iowa State University of Science and Technology
Ph.D., 1961
Chemistry, physical

University Microfilms, Inc., Ann Arbor, Michigan

THE CRYSTAL STRUCTURE OF BISMUTH MONOCHLORIDE

by

Alexander Hershaft

A Dissertation Submitted to the
Graduate Faculty in Partial Fulfillment of
The Requirements for the Degree of
DOCTOR OF PHILOSOPHY

Major Subject: Inorganic Chemistry

Approved:

Signature was redacted for privacy.

In Charge of Major Work

Signature was redacted for privacy.

Head of Major Department

Signature was redacted for privacy.

Dean of Graduate College

Iowa State University
Of Science and Technology
Ames, Iowa

1961

TABLE OF CONTENTS

	Page
INTRODUCTION	1
The Problem--Solution of Bismuth in Liquid Bismuth Trichloride	1
The Story of BiCl and Related Compounds	4
EXPERIMENTAL PROCEDURE	7
Preparation of Crystals	7
Determination of Density	10
Diffraction Data	14
Treatment of Intensities	16
STRUCTURE DETERMINATION	20
Vector Maps	20
Calculation of Structure Factors	36
Electron Density Maps	40
STRUCTURE REFINEMENT AND FUNCTIONAL ANALYSIS	47
Refinement of Structure	47
Weighting of Intensities	52
Functional Analysis	56
DISCUSSION	60
Interpretation of Structure	60
Reliability of Model	62
Conclusions	65
SUMMARY	68
LITERATURE CITED	70
ACKNOWLEDGEMENTS	73
APPENDIX A: COMPUTER PROGRAMS	75
Absorption Correction and Sharpening Program	75
Standard Deviations Program	81
APPENDIX B: OBSERVED AND CALCULATED STRUCTURE FACTORS	86

To the memory of my father whose exemplary life and untimely
martyrdom provided the original stimulus and

To my mother who sentenced herself to ten years of solitude
in order that I may attain this height of academic achieve-
ment.

INTRODUCTION

The Problem--Solution of Bismuth in
Liquid Bismuth Trichloride

Solutions of metals in their molten salts are of current interest because of unanswered questions concerning the mechanism of solution and the type of species which are formed. Contributions to a better understanding of these solutions have been made through measurements of vapor pressures, phase equilibria, freezing point depressions, electrical properties, and absorption spectra. Still, the species and equilibria in solution are not defined adequately and there exist at present almost as many pet theories as there are men of science who have given of their time and effort to the problem.

The three principal models currently being considered for solution mechanism involve the formation of (1) neutral metal atoms or molecules, (2) metal ions plus solvated electrons, or (3) reduced ions or molecules. The last view, credited with the greatest degree of support, has been championed vigorously by Corbett (Corbett et al., 1957; Corbett, 1961). The Bi-BiCl₃ system is of particular interest in this connection because the reduced salt, identified as bismuth monochloride*

*The term "bismuth monochloride" and the symbol BiCl will be used throughout this work for the sake of convenience to designate the compound whose crystallographic formula turns out to be BiCl_{1.17}.

precipitates out of solution as a solid phase.

Cubicciotti, the major exponent of the first two theories (Cubicciotti, 1952, 1960a; Keneshea and Cubicciotti, 1958), argued that positive deviations from Raoult's law in the Bi-BiCl₃ system deny the existence of individual lower valent ions in solution (Cubicciotti et al., 1958). He acknowledged, however, that reduced polymeric ions like Bi_n^{+m} would fit his data for the vapor pressure of Bi dissolved in BiCl₃. According to Cubicciotti, Bi atoms or ions, upon solution, enter the octahedral holes in the quasi-lattice of the molten chloride.

The cryoscopic data of Mayer et al. (1960) indicated Bi₂Cl₂ as the principal constituent of moderately concentrated solutions near the BiCl₃ liquidus curve. Concurrently, Bredig (1959) proposed the presence of both the Bi₂ and Bi₂Cl₂ species, with the former becoming more prevalent at high temperatures, to reconcile the vapor pressure and cryoscopic results. Yosim et al. (1959) noted that the presence of neutral dimers or Bi₂⁺⁺ ions is consistent with electrical conductivity, vapor pressure and magnetic susceptibility measurements. They also pointed out, however, that no single species or mechanism is sufficient to explain the entire phase diagram and particularly the retrograde solubility above the syntectic temperature.

More recently, Topol et al. (1961) studied the Bi-BiCl₃

system by e.m.f. measurements. They observed a Nernst $n = 2$, corresponding to the species BiCl , at low metal concentrations ($N_2 < .01$), whereas slightly higher concentrations yielded n values of 6 and even 8. The authors concluded that both BiCl (or Bi^+) and Bi_4Cl_4 are likely to be present in solution, the latter becoming predominant with increasing Bi concentration. The presence of other species such as Bi_2 , Bi_3Cl_3 and Bi_3^+ was not excluded.

Interpretation of thermodynamic data in fused salt systems for the purpose of identifying the species formed involves broad assumptions about such concepts as activity coefficients and formation of solid solutions and it is not surprising that attempts along this line have met with rather limited success. The more direct, physical methods have been showing greater promise. Already the discovery of the diamagnetic character of these solutions has narrowed considerably the range of possible species.

More recently, two structural studies made significant contributions to the available evidence. Measurement of the visible absorption spectra by Boston and Smith (1960) provided first direct evidence for the existence of two species in solution. Although these have not been positively identified, it appears that the species prevalent at very low bismuth concentrations (0.01 M) was the Bi atom or the Bi^+ ion. This is consistent with Holecek's (1953) observation that magnetic

susceptibility increases with decreasing metal concentration in this concentration region. The second study, by Levy et al. (1960), in the form of x-ray diffraction on molten and crystalline BiAlCl_4 apparently indicates the presence of Bi_3^{+3} ions in both phases.

Although no definite conclusions have been reached at this stage, certain general notions have transpired. The formation of several reduced species has been pretty well established. Furthermore, it appears very likely that these species are Bi^+ or BiCl at very low metal concentrations with some degree of polymerization taking place as the bismuth content is increased. An approach more direct and complete than any tried before was definitely indicated at this stage. Just as inspection of fossilized remains in ancient rocks gave man his first glimpse of early life forms, vital clues to the nature of the solute species were expected from a study of their frozen equilibrium in a crystal structure.

The Story of BiCl and Related Compounds

In 1908, Eggink presented the first substantial characterization of the Bi-BiCl_3 system in the form of a phase diagram. He observed that when the two-liquid phase obtained with excess metal was cooled, an intermediate solid phase separated at a temperature higher than the melting point of either component. Eggink's claim of isolating BiCl by

ether extraction of the trichloride from the mixture has since been questioned by Corbett (1958).

Some 40 years later, Sokolova (1952) redetermined the Bi-BiCl₃ phase diagram and, subsequently, reported x-ray and microstructure observations on the system, (Sokolova et al., 1954). With the aid of powder patterns she detected the new phase in quenched Bi-BiCl₃ solutions and claimed for it the BiOCl structure on the basis of similar intensity distributions.

The third and most thorough study was due to Yosim et al. (1959) who published the complete phase diagram for the system. As Eggink and Sokolova before them, they recognized the presence of an intermediate phase with an approximate BiCl stoichiometry but made no attempt to isolate it.

The elusive monohalide was finally cast into the limelight by Corbett (1958) who isolated the compound and described its properties in some detail. Subsequently, Darnell and Yosim (1959) presented a thermodynamic characterization of solid BiCl and Cubicciotti (1960b) reported equilibrium data for BiCl gas. Corbett's preliminary powder pattern data agreed well with those deduced by Holecek (1953) but bore little resemblance to the patterns reported by Sokolova et al. It appears likely that the presence of hydration and hydrolysis products was responsible for the discrepancy and for the presence of BiOCl lines in her powder

patterns. On the basis of certain properties of BiCl such as its diamagnetic character and the high viscosity of its solutions, Corbett predicted cyclic polymerization in the crystal.

Wolten and Mayer (1958) were able to index powder patterns of BiCl₃ on the basis of a primitive cubic unit cell with $a_0 = 8.14 \text{ \AA}$ and space group P2₁3. Concurrent calculations based on BiCl powder patterns led Wolten* to claim a hexagonal unit cell for the monohalide. In the vapor phase, BiCl₃ was found to consist of pyramidal molecules with a Bi-Cl bond length of 2.48 \AA and a Cl-Bi-Cl angle of $\sim 100^\circ$ (Skinner and Sutton, 1940). Levy et al. (1959) found from x-ray diffraction studies of molten, polycrystalline and monocrystalline BiAlCl₄ that the Bi atoms apparently form equilateral triangles with a Bi-Bi bond length of 3.04 \AA . Solid BiAlCl₄ crystallizes in the rhombohedral system with $a_0 = 12.12 \text{ \AA}$, $\alpha = 58^\circ 23'$, $Z = 6$ and space group R3c, which conveniently accommodates 2 Bi_3^{+3} units.

In closing, mention should be made of the compound Bi₂₄O₃₁Cl₁₀ for which the chief connection with this work lies in its outsized unit cell. An idealized model for this structure was proposed by Sillen and Edstrand (1942). The model featured 24 Bi atoms in a unit cell of approximately $30 \times 10 \times 4 \text{ \AA}$. Bi-Cl bond lengths of 3.30 \AA and 3.45 \AA were measured.

* Wolten, G. M., Atomics International, Canoga Park, California. Powder patterns of BiCl. Private communication. 1958.

EXPERIMENTAL PROCEDURE

Preparation of Crystals

Preparation of bismuth monochloride has been described by Corbett (1958). Mixtures containing up to 76% BiCl were synthesized by equilibration of BiCl₃ with excess metal at 325° in a sealed Pyrex tube, followed by the reduction of temperature to 270° over a period of one to two weeks. Each time, the tube was opened in an inert atmosphere and single crystals of BiCl projecting from the matrix were picked out manually. Over 100 crystals were obtained in this manner.

BiCl crystallizes in the form of shiny black prisms with a flattened hexagonal cross section. Upon contact with the atmosphere, signs of surface decomposition became evident within two days. After 10 days of exposure, deterioration of the crystals had progressed to the stage where diffraction would be no longer practical. Figure 1 shows some of the larger specimens found. The surfaces bear traces of the hydrolyzed matrix which was removed during the shaping operation.

Because of the high absorption coefficient of Bi atoms, the crystals had to be ground into regular shapes in order that a convenient and accurate absorption correction could be applied to the observed diffraction intensities. Cylindrical shapes were attained by rolling crystals over fine emery

Figure 1. Crystals of BiCl_3 ; the largest specimen measures
136 x 368 x 1670 μ



paper with the bare finger. One of these cylinders is shown in Figure 1. Spheres were prepared with the aid of a circular abrasive track patterned after Bond (1951).

Some 25 cylindrical and spherical crystals of diverse size and degree of regularity were mounted in hand drawn, evacuated capillaries. This precaution insured that all diffraction data could be taken with the same crystal. Preliminary Weissenberg photographs were taken of each crystal and the most suitable specimen was selected on the basis of dimensional uniformity, intensity and neatness of reflection spots, and alignment with the axis of rotation. Spheres were rejected en masse because they produced weak reflections with extensive smudging.

Optimum thickness for the diffraction specimen was originally calculated according to Buerger's (1942, p. 180) formula $t = 2/\mu$, where t is the thickness of the crystal and μ is the linear absorption coefficient. The value $t = 2/1513 = .0013$ cm, thus obtained, was found unsatisfactory during the preliminary diffraction exposures and a cylinder .0320 cm long with a diameter of .0098 cm was eventually selected.

Determination of Density

Determination of the experimental density of BiCl presented a special problem because the crystals were too heavy for the floatation technique and too scarce for the macro-

pycnometric method. Corbett* had obtained a macro-pycnometric value of 6.54 g/cc by measuring the density of a BiCl-BiCl₃ mixture and correcting for a small trichloride impurity. Since this value did not agree with the assumed stoichiometry of the crystal, it was decided to experiment with two other more direct approaches.

The dimensions of seven of the largest regularly shaped crystals were carefully measured under a binocular microscope and their weights were determined on a microbalance by Mr. Robert Bachman of the Ames Laboratory. Their average density of 6.05 g/cc was considered unreliable because of considerable variation among individual determinations and the likelihood that surface imperfections made this value too low.

Subsequent efforts to measure density by weighing crystals in air and in heavy liquid failed, giving way to the development of a micropycnometric approach which offered very good precision while requiring only several milligrams of material. The apparatus employed in the micropycnometric technique is shown in Figure 2. The micropycnometer can be conveniently manufactured from capillary tubing. After its volume had been determined by the conventional method, the

*Corbett, J. D., Department of Chemistry, Iowa State University of Science and Technology, Ames, Iowa. Determination of the density of BiCl. Private communication. 1958.

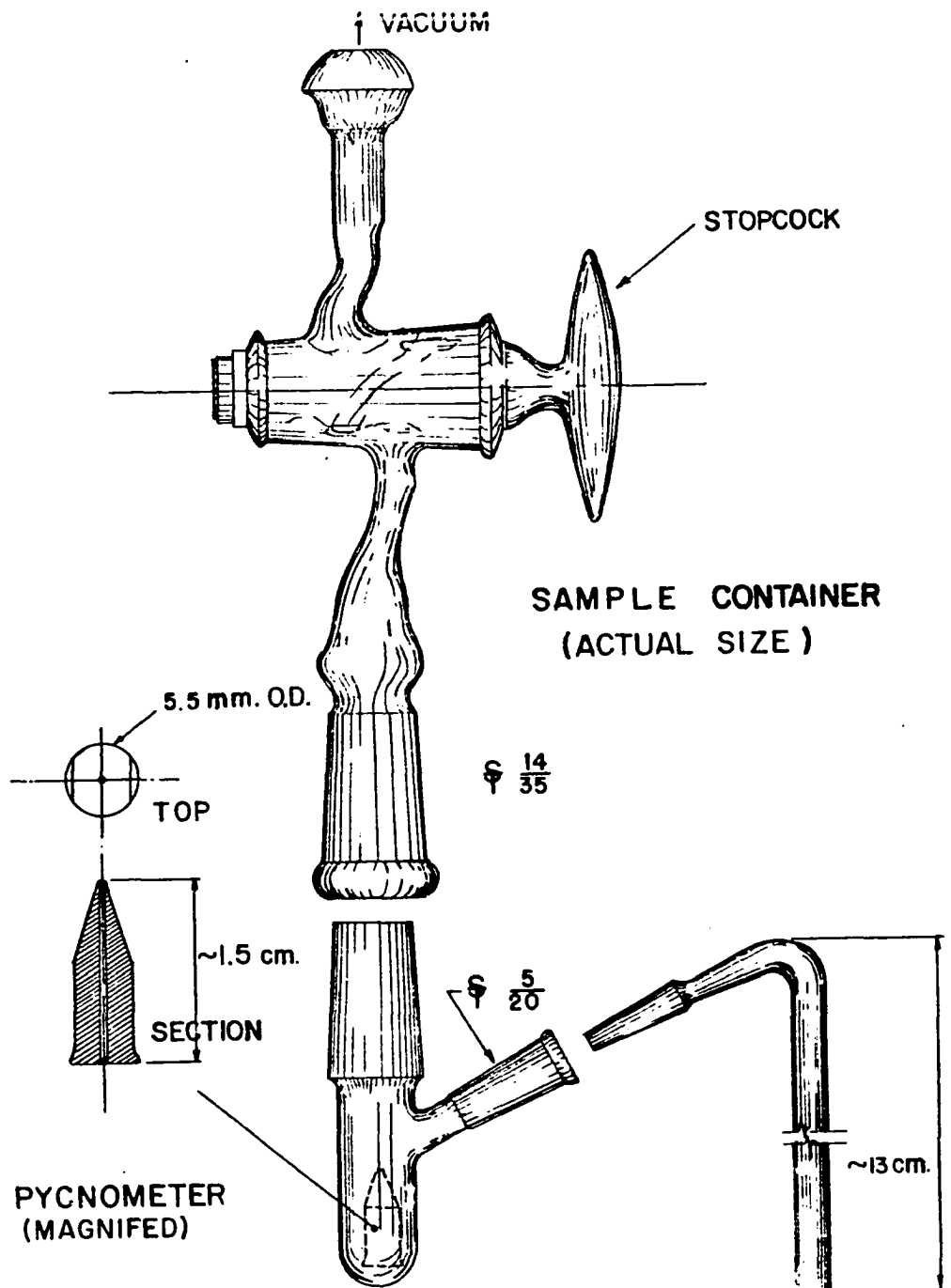


Figure 2. Micropycnometric density apparatus

pycnometer was cleaned, weighed on a microbalance, loaded with crystals, and reweighed. This assembly was then placed in the sample container and the side arm was filled with 1-bromonaphthalene, selected for its low vapor pressure and chemical inertness. The density of 1-bromonaphthalene was measured with the same pycnometer, and found to be $1.4997 \pm .003$ g/cc at 25° as compared with the literature value of 1.4785 g/cc (Jones and Lapworth, 1914). The sample container was evacuated to remove all traces of air from the crystals and liquid alike, following which 1-bromonaphthalene was allowed to enter the pycnometer by turning the side arm upward. In the last step, the micropycnometer containing crystals and liquid was removed from the sample container, wiped clean, and weighed.

Calculations were carried out according to the formula

$$\rho_c = \frac{w_c}{V_p \rho_l - \frac{w_{c+l}}{\rho_l} + w_c} \rho_l$$

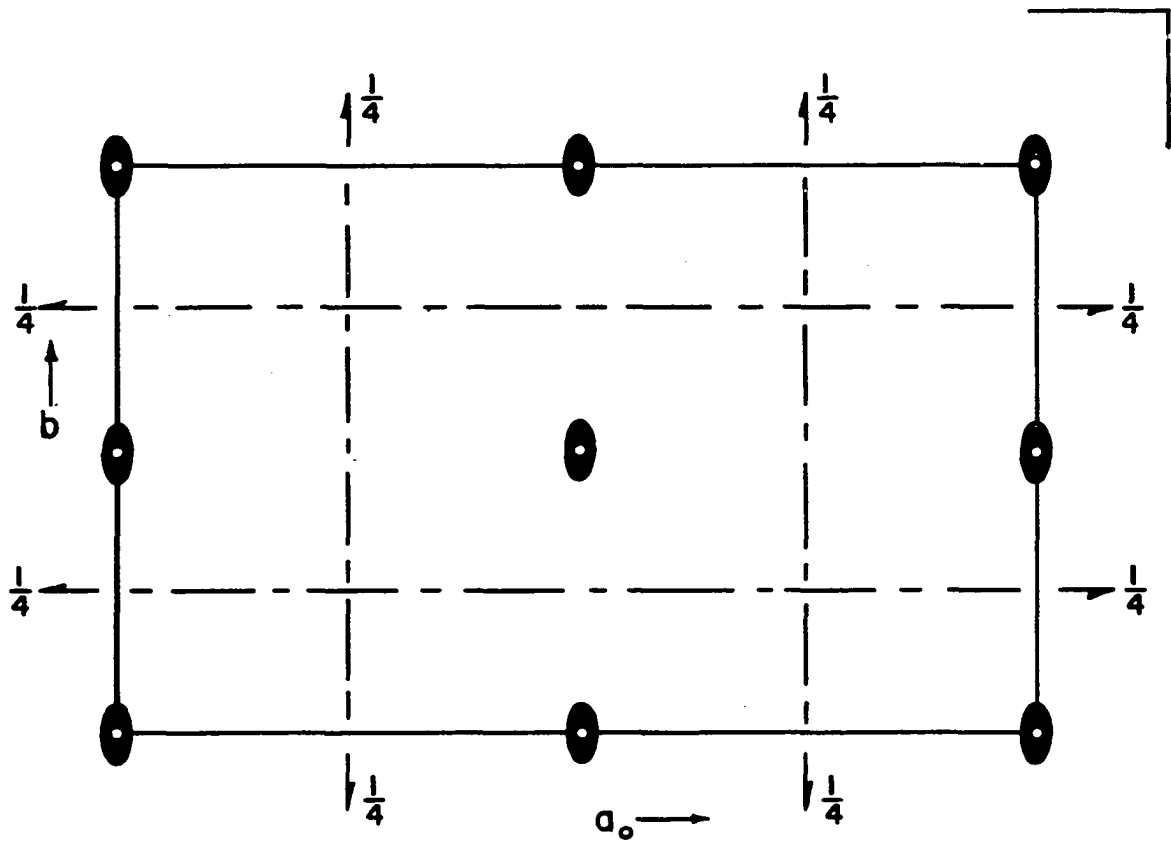
where the symbols ρ , w , and v denote density, weight, and volume and the subscripts p , c , and l refer to pycnometer, crystals, and liquid, respectively. Individual determinations were made on five batches of crystals. Their average value of $6.54 \pm .05$ g/cc was identical with Corbett's result and was accepted as the true density of BiCl .

Diffraction Data

Preliminary Weissenberg and precession photographs indicated an orthorhombic unit cell. Lack of systematic extinctions for the hkl and $hk0$ data in conjunction with the extinction conditions $h + l = 2n + 1$ for $h0l$ data and $k + l = 2n + 1$ for Ok_l data, allowed the choice of space groups Pnn and $Pnmm$. Figure 3 illustrates the location of symmetry elements in space group $Pnmm$ and lists the general coordinates of the two symmetry sets allowed by extinction rules.

Precision lattice constants were measured by the conventional Weissenberg back reflection method (Buerger, 1942) using unfiltered Cu, Cr, and Co radiation. Their values were $a_0 = 23.057 \pm .002 \text{ \AA}$, $b_0 = 15.040 \pm .007 \text{ \AA}$, c_0 (the needle axis) $= 8.761 \pm .003 \text{ \AA}$. On this basis, 48 BiCl molecules per unit cell were most likely, resulting in a calculated density of 6.41 g/cc.

All intensity data were taken with Cu $K\alpha$ radiation. A molybdenum target could not be used because it produced fluorescence in bismuth. Multiple film Weissenberg photographs were taken for layers $hk0$, hkl , $hk2$, $hk3$, $hk4$, $hk5$ by the equi-inclination technique (Buerger, 1942). Exposure times varied between 120 and 180 hours. Precession exposures of 2, 4, 8, 16, and 32 hours were taken of layers $h0l$, hll , and Ok_l in order to supplement the Weissenberg data at low



8 — FOLD POSITIONS

$$x, y, z; \bar{x}, \bar{y}, z; \frac{1}{2}+x, \frac{1}{2}-y, \frac{1}{2}-z; \frac{1}{2}-x, \frac{1}{2}+y, \frac{1}{2}-z;$$

$$\bar{x}, \bar{y}, \bar{z}; x, y, \bar{z}; \frac{1}{2}-x, \frac{1}{2}+y, \frac{1}{2}+z; \frac{1}{2}+x, \frac{1}{2}-y, \frac{1}{2}+z;$$

4 — FOLD POSITIONS

$$x, y, 0; \bar{x}, \bar{y}, 0; \frac{1}{2}+x, \frac{1}{2}-y, \frac{1}{2}; \frac{1}{2}-x, \frac{1}{2}+y, \frac{1}{2}.$$

Figure 3. Symmetry elements and general coordinates of space group Pnm

angles.

Weissenberg films were judged visually against series of standard spots prepared separately for each layer to allow for wear and changing spot shape. The film factor was checked against visual observations and adjusted in accordance with spot intensity. Reflections appearing on different films in a pack were double checked until their observed values agreed within 10% or less. For each layer, uniform portions of the reciprocal lattice were exposed on a single film pack to provide a basis for converting all Weissenberg intensities to the same relative scale. Precession reflections were judged against a selected spot appearing on the $h0l$ films. These were subsequently brought in line with the rest of the data by comparing intensities of reflections common to Weissenberg and precession films. In all, 1938 observed reflections were judged. The 566 unobserved reflections, which were not subject to systematic extinctions, were assigned a value equal to 60% of the lowest observable intensity for that layer. Table 1 lists the number of reflections obtained for each layer.

Treatment of Intensities

Before the observed intensities could be used in structure determination, they had to be corrected for the Lorentz factor, polarization, absorption, and multiplicity.

Lorentz and polarization corrections were applied to the

Table 1. Number of reflections

Layer	Weissenberg observed	Reflections unobserved	Precession reflections	Total reflections
hk0	357	89	3	449
hk1	338	101	6	445
hk2	330	103	5	438
hk3	312	106	3	421
hk4	308	81	4	393
hk5	287	68	3	358
Total	1932	548	24	2504

Weissenberg intensities by means of the I.B.M. 650 computer using INCOR-IM, a locally-modified version of the INCOR-I program (Zalkin and Jones, 1957). Precession data were handled with the aid of Olson's* correction program.

A new approach to the calculation of absorption corrections was recently presented by Bond (1959) ending Bradley's (1935) 24 year hegemony in this field. Figure 4 illustrates the marked discrepancy between the two treatments. An absorption correction and sharpening (ACS) program, based in part on Bond's paper, was written for the I.B.M. 650 computer.

* Olson, D. H., Department of Chemistry, Iowa State University of Science and Technology, Ames, Iowa. Correction program for precession intensities. Private communication. 1960.

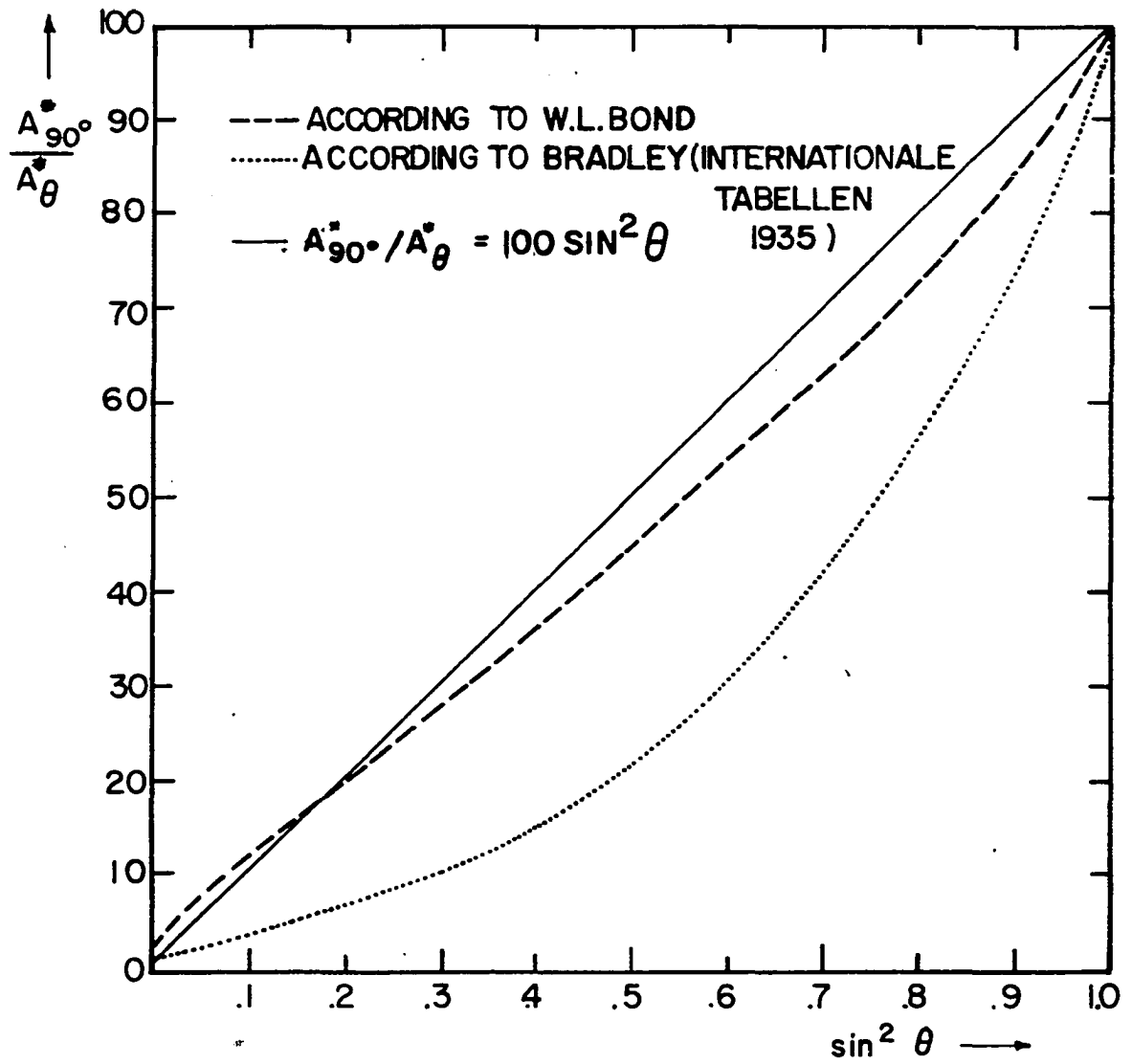


Figure 4. Absorption correction plots; $\mu R = 8.0$

The program is designed to apply absorption corrections to Weissenberg data from cylindrical and spherical crystals and to "sharpen" intensities according to the method proposed by Patterson (1935) and developed by Lipson and Cochran (1957, p. 170). A detailed program writeup is given in Appendix A.

Absorption corrections are listed in Bond's paper as a function of θ and μR , where θ is the Bragg angle and μ is the linear absorption coefficient. R is defined by the relation

$$R = R_0 \sec \nu,$$

where ν is the angle between the incident x-ray beam and a plane normal to the cylinder axis. In the present case, $\mu = 1513 \text{ cm}^{-1}$ and $R_0 = 9.8 \times 10^{-3} \text{ cm}$, so that $R = 7.4 \sec \nu$.

Plots of absorption correction vs. $\sin^2\theta$ were prepared for different values of μR , as required by the program, and corrected intensities were computed for all Weissenberg reflections by means of the ACS program. Absorption-corrected precession intensities were read off a plot of W_{LPA}/P_{LP} vs. $\sin^2\theta$, where W and P stand for Weissenberg and precession intensities and L , P , and A indicate that the Lorentz, polarization, and absorption corrections have been applied. The conversion of all intensities to the same scale took place during this step.

Division by the appropriate multiplicity factors was accomplished during the routine operations prior to the summation of the Fourier series.

STRUCTURE DETERMINATION

The approach to structure determination was based on the "heavy atom" technique. This assumes that the correct assignment of bismuth positions will establish the phase angles of most large reflections and thus lead to the determination of chlorine positions by Fourier methods.

Trial structures were based on interpretation of Patterson vector maps. Conventional and difference Fourier maps were employed to locate chlorine atoms.

Vector Maps

The general form of the Patterson function is

$$P(XYZ) = \frac{1}{V} \sum_h \sum_k \sum_{l=-\infty}^{\infty} F(hkl)^2 \exp 2\pi i(hX+kY+lZ),$$

where X, Y, and Z designate grid points of the unit cell rather than atomic coordinates, V is the volume of the unit cell, and F is a quantity to be discussed later, known as the structure factor. In space group Pnm, the relation $F(hkl) = F(\bar{h}k\bar{l}) = F(h\bar{k}l) = F(hk\bar{l})$ holds for all reflections. Consequently, the above expression reduces to

$$P(XYZ) = \frac{8}{V} \sum_h \sum_k \sum_{l=0}^{\infty} F(hkl)^2 \cos 2\pi hX \cos 2\pi kY \cos 2\pi lZ$$

or, more specifically, to

$$\begin{aligned}
P(XYZ) = & \frac{1}{V} F^2(000) + \frac{2}{V} \left[\sum_{h=1}^{\infty} F^2(h00) \cos 2\pi hX \right. \\
& + \sum_{k=1}^{\infty} F^2(0k0) \cos 2\pi kY + \left. \sum_{l=1}^{\infty} F^2(00l) \cos 2\pi lZ \right] \\
& + \frac{4}{V} \left[\sum_h \sum_{k=1}^{\infty} F^2(hk0) \cos 2\pi hX \cos 2\pi kY \right. \\
& + \sum_h \sum_{l=1}^{\infty} F^2(h0l) \cos 2\pi hX \cos 2\pi lZ \\
& + \left. \sum_k \sum_{l=1}^{\infty} F^2(0kl) \cos 2\pi kY \cos 2\pi lZ \right] \\
& + \frac{8}{V} \left[\sum_h \sum_k \sum_{l=1}^{\infty} F^2(hkl) \cos 2\pi hX \cos 2\pi kY \cos 2\pi lZ \right].
\end{aligned}$$

As the first step, a sharpened $hk0$ Patterson projection was computed and plotted since, up to that point, the only indication of the complexity of the structure was the large volume of the unit cell for a compound with an apparently simple stoichiometry. The form of the two-dimensional function is

$$\begin{aligned}
P(XY0) = & \frac{1}{A} F^2(000) + \frac{2}{A} \left[\sum_{h=1}^{\infty} F^2(h00) \cos 2\pi hX \right. \\
& + \left. \sum_{k=1}^{\infty} F^2(0k0) \cos 2\pi kY \right] + \frac{4}{A} \left[\sum_h \sum_{k=1}^{\infty} F^2(hk0) \cos 2\pi hX \right. \\
& \left. \cos 2\pi kY \right]
\end{aligned}$$

The 360 observed $hk0$ intensities were multiplied by means of

the ACS program by the sharpening factor $(\sum_j Z_j / \sum_j f_j)^2$ where Z_j is the atomic number and f_j , the dispersion-corrected scattering factor of atom j . The summing code specifying the evenness or oddness of indices was supplied and special reflections were divided by their appropriate multiplicity factors.

Summation was performed on the I.B.M. 650 computer using the TDF-2 program (Fitzwater and Williams, 1959). Results were tabulated on the I.B.M. 420 tabulator with the aid of a special wiring panel which expands the basic $\frac{1}{4} \times \frac{1}{4} \times \frac{1}{4}$ portion of the unit cell into the desired $\frac{1}{2} \times \frac{1}{2} \times \frac{1}{2}$ octant. The *mmm* symmetry of the vector map made it unnecessary to consider the entire unit cell. A contour map of the sharpened *hk0* Patterson projection is shown in Figure 5.

The vectors which these peaks represent were classified as intraset or interset according to whether they referred to atoms of the same or different symmetry sets. The mode of attack consisted of the selection of possible Bi positions on the basis of intraset vectors, and subsequent use of interset vectors for verification. The general coordinates of intraset and interset vectors, based on the four-fold set of Figure 3, are listed in Tables 2 and 3 along with their respective multiplicities.

The major peaks along the right hand edge and the upper edge of the vector map were very likely to represent in part

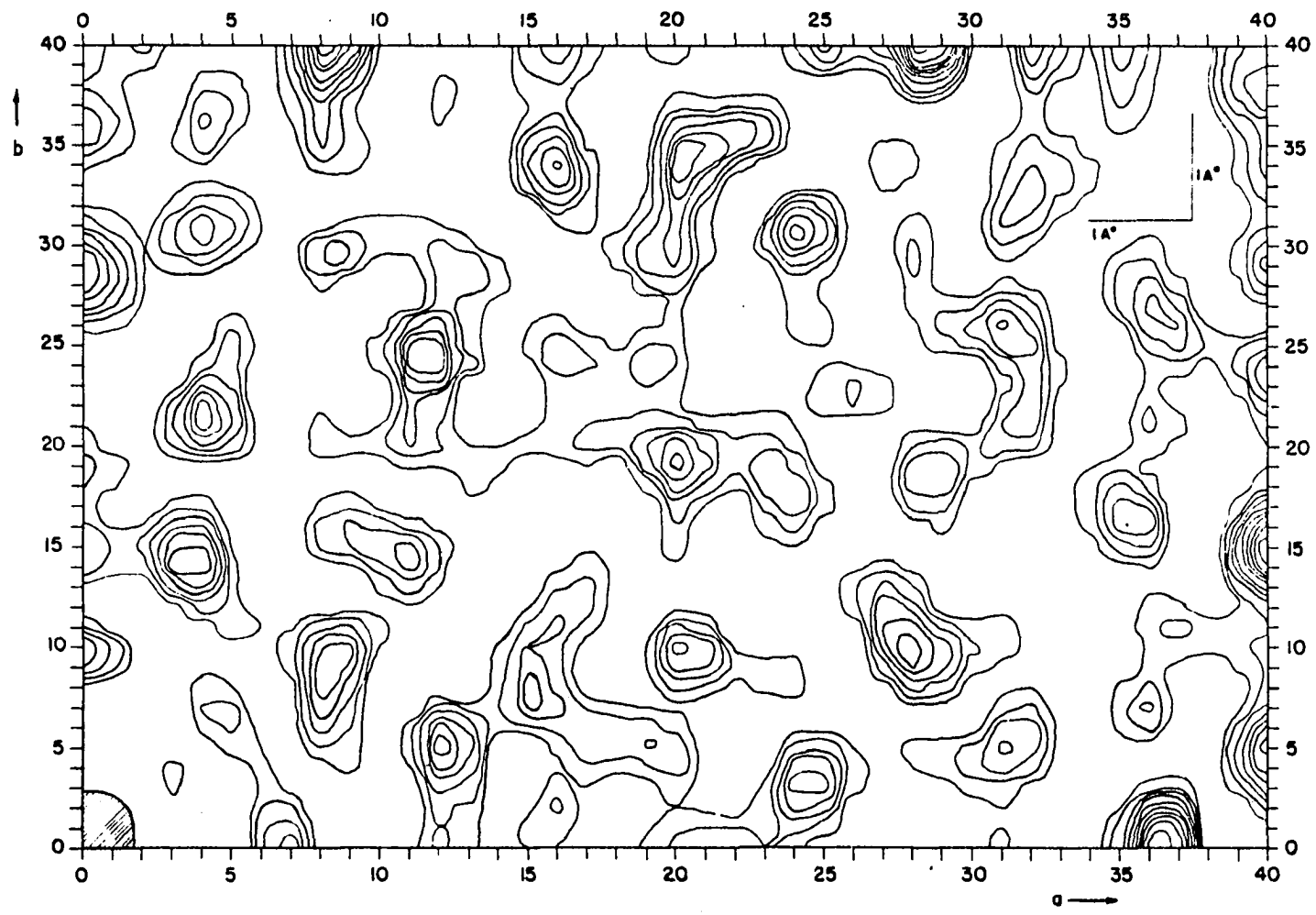


Figure 5. Sharpened Patterson projection onto the (001) plane

Table 2. Intraset vectors

Vectors				Multiplicity	
				8-fold	4-fold
0	0	0		8	4
0	0	$\pm 2z$		4	
$\pm 2x$	$\pm 2y$	0		2	1
$\pm 2x$	$\bar{\pm} 2y$	0		2	1
$\pm 2x$	$\pm 2y$	$\pm 2z$		1	
$\pm 2x$	$\pm 2y$	$\bar{\pm} 2z$		1	
$\pm 2x$	$\bar{\pm} 2y$	$\pm 2z$		1	
$\pm 2x$	$\bar{\pm} 2y$	$\bar{\pm} 2z$		1	
$\frac{1}{2}\pm 2x$	$\frac{1}{2}$	$\frac{1}{2}$		4	2
$\frac{1}{2}\pm 2x$	$\frac{1}{2}$	$\frac{1}{2}\pm 2z$		2	
$\frac{1}{2}\pm 2x$	$\frac{1}{2}$	$\frac{1}{2}\bar{\pm} 2z$		2	
$\frac{1}{2}$	$\frac{1}{2}\pm 2y$	$\frac{1}{2}$		4	2
$\frac{1}{2}$	$\frac{1}{2}\pm 2y$	$\frac{1}{2}\pm 2z$		2	
$\frac{1}{2}$	$\frac{1}{2}\pm 2y$	$\frac{1}{2}\bar{\pm} 2z$		2	

Table 3. Interset vectors. Δz and Σz transform to z for vectors between 8- and 4-fold sets and to 0 for vectors between 4- and 4-fold sets; each vector has a multiplicity of 2

Vectors			Vectors		
$\underline{+\Delta x}$	$\underline{+\Delta y}$	$\underline{+\Delta z}$	$\frac{1}{2}\underline{+\Delta x}$	$\frac{1}{2}\underline{+\Delta y}$	$\frac{1}{2}\underline{+\Delta z}$
$\underline{+\Delta x}$	$\underline{+\Delta y}$	$\bar{+\Delta z}$	$\frac{1}{2}\underline{+\Delta x}$	$\frac{1}{2}\underline{+\Delta y}$	$\frac{1}{2}\bar{+\Delta z}$
$\underline{+\Delta x}$	$\bar{+\Delta y}$	$\underline{+\Delta z}$	$\frac{1}{2}\underline{+\Delta x}$	$\frac{1}{2}\bar{+\Delta y}$	$\frac{1}{2}\underline{+\Delta z}$
$\underline{+\Delta x}$	$\bar{+\Delta y}$	$\bar{+\Delta z}$	$\frac{1}{2}\underline{+\Delta x}$	$\frac{1}{2}\bar{+\Delta y}$	$\frac{1}{2}\bar{+\Delta z}$
$\underline{+\Delta x}$	$\underline{+\Delta y}$	$\underline{+\Sigma z}$	$\frac{1}{2}\underline{+\Sigma x}$	$\frac{1}{2}\underline{+\Delta y}$	$\frac{1}{2}\underline{+\Sigma z}$
$\underline{+\Delta x}$	$\underline{+\Delta y}$	$\bar{+\Sigma z}$	$\frac{1}{2}\underline{+\Sigma x}$	$\frac{1}{2}\underline{+\Delta y}$	$\frac{1}{2}\bar{+\Sigma z}$
$\underline{+\Delta x}$	$\bar{+\Delta y}$	$\underline{+\Sigma z}$	$\frac{1}{2}\underline{+\Sigma x}$	$\frac{1}{2}\bar{+\Delta y}$	$\frac{1}{2}\underline{+\Sigma z}$
$\underline{+\Delta x}$	$\bar{+\Delta y}$	$\bar{+\Sigma z}$	$\frac{1}{2}\underline{+\Sigma x}$	$\frac{1}{2}\bar{+\Delta y}$	$\frac{1}{2}\bar{+\Sigma z}$
$\underline{+\Sigma x}$	$\underline{+\Sigma y}$	$\underline{+\Sigma z}$	$\frac{1}{2}\underline{+\Sigma x}$	$\frac{1}{2}\underline{+\Delta y}$	$\frac{1}{2}\underline{+\Sigma z}$
$\underline{+\Sigma x}$	$\underline{+\Sigma y}$	$\bar{+\Sigma z}$	$\frac{1}{2}\underline{+\Sigma x}$	$\frac{1}{2}\underline{+\Delta y}$	$\frac{1}{2}\bar{+\Sigma z}$
$\underline{+\Sigma x}$	$\bar{+\Sigma y}$	$\underline{+\Sigma z}$	$\frac{1}{2}\underline{+\Sigma x}$	$\frac{1}{2}\bar{+\Delta y}$	$\frac{1}{2}\underline{+\Sigma z}$
$\underline{+\Sigma x}$	$\bar{+\Sigma y}$	$\bar{+\Sigma z}$	$\frac{1}{2}\underline{+\Sigma x}$	$\frac{1}{2}\bar{+\Delta y}$	$\frac{1}{2}\bar{+\Sigma z}$
$\underline{+\Sigma x}$	$\underline{+\Sigma y}$	$\underline{+\Delta z}$	$\frac{1}{2}\underline{+\Delta x}$	$\frac{1}{2}\underline{+\Sigma y}$	$\frac{1}{2}\underline{+\Sigma z}$
$\underline{+\Sigma x}$	$\underline{+\Sigma y}$	$\bar{+\Delta z}$	$\frac{1}{2}\underline{+\Delta x}$	$\frac{1}{2}\underline{+\Sigma y}$	$\frac{1}{2}\bar{+\Sigma z}$
$\underline{+\Sigma x}$	$\bar{+\Sigma y}$	$\underline{+\Delta z}$	$\frac{1}{2}\underline{+\Delta x}$	$\frac{1}{2}\bar{+\Sigma y}$	$\frac{1}{2}\underline{+\Sigma z}$
$\underline{+\Sigma x}$	$\bar{+\Sigma y}$	$\bar{+\Delta z}$	$\frac{1}{2}\underline{+\Delta x}$	$\frac{1}{2}\bar{+\Sigma y}$	$\frac{1}{2}\bar{+\Sigma z}$

the intraset vectors $\frac{1}{2}, \frac{1}{2}+2y, 0$ and $\frac{1}{2}+2x, \frac{1}{2}, 0$, respectively. The positions of these peaks were thus used to compile a list of possible x and y values which were subsequently paired by checking for the presence of corresponding $2x, 2y, 0$ peaks within the body of the map. The characteristic Patterson ambiguity due to the four possible sign combinations was resolved by arbitrarily assigning one position as the site of a reference Bi atom from the set of four which was derived from the strongest and best defined vector peaks. This fixed the origin of the unit cell and provided a basis for interset verification.

Some 40 independent positions satisfied the interset requirements listed in Table 3 with respect to the reference atom. The task at hand was to select at least five from amongst these which would satisfy all interset requirements with respect to each other as well. Six independent positions could generate the minimum number of (eight-fold) symmetry sets required.

To this end, all 40 positions were listed in table form and the presence or absence of peaks corresponding to interset vectors was noted for each pair. The search for a self-consistent group of positions was conducted according to a systematic and efficient procedure developed especially for this purpose. Still, the large degree of overlap of projected electron densities and the reduction in the number of

checks due to the lack of z parameters soon rendered the task highly impractical.

In order to overcome these handicaps, it was decided to tackle the problem via a sharpened three-dimensional Patterson map. The procedure for obtaining corrected three-dimensional data has been described in the experimental section. A total of 1956 observed reflections was used in the summation. Sharpening and other preliminary operations were performed in the manner outlined for the two-dimensional case. Computation times for the different permutations of indices and grid dimensions were calculated and the sequences h, k, l and 1/80, 1/40, 1/40 were selected. Summation was again performed on the I.B.M. 650 computer using the TDF-2 program but this time the I.B.M. 407 tabulator was used to tabulate and print the results directly on a grid suitable for plotting contours. This last step saved the time of copying hundreds of thousands of electron density values by hand.

An absolute scale factor k (such that $F_o \cdot \sqrt{k} = F_c$) and an average temperature factor B (such that $f = f_o \exp -B \frac{\sin^2 \theta}{\lambda^2}$) were evaluated from a plot of $\log \langle F_o^2 / \Sigma f_o^2 \rangle$ vs. $\langle \frac{\sin^2 \theta}{\lambda^2} \rangle$ according to the relation

$$\log \left\langle \frac{F_o^2}{\Sigma f_o^2} \right\rangle = \log \frac{1}{k} - \frac{2B}{2.303} \left\langle \frac{\sin^2 \theta}{\lambda^2} \right\rangle$$

derived by Wilson (1942). These were found to be $\frac{1}{8} \sqrt{k} = 12.2$

(for 1/8 of the unit cell) and $B = 2.72 \text{ cm}^2$. The height of the Patterson origin peak was calculated by two approaches using these values of k and B . This led to the assignment of experimental peak heights to the interatomic vectors and to the conversion of the $F^2(000)$ term to the "floor" value.

In computing the Patterson synthesis it is customary to neglect the $F^2(000)$ term and the $8/V$ factor. Consequently, the relation between the theoretical and the experimental Patterson functions is expressed by

$$P_{\text{theo}}(\text{XYZ}) = \frac{8}{V} k P_{\text{exp}} + \frac{1}{V} F^2(000).$$

$F^2(000)$ can be calculated from the definition of a structure factor:

$$F(hkl) = \sum_{n=1} f_n \exp 2\pi i (hx_n + ky_n + lz_n),$$

so that

$$F^2(000) = \sum_{n=1} f_n^2 = [48(18+78)]^2 = 2.074 \times 10^7.$$

Since $V = 23.057 \cdot 15.040 \cdot 8.761 \text{ \AA}^3 = 3038 \text{ \AA}^3$, $k = (8 \cdot 12.2)^2 = 9.5 \cdot 10^3$, and $P_{\text{exp}}(000) = 27,150$, the theoretical height of the origin peak is given by

$$\begin{aligned} P_{\text{theo}}(000) &= \frac{8}{3038} \cdot 9.5 \cdot 10^3 \cdot 27,150 + \frac{1}{3038} \cdot 2.079 \cdot 10^7 \\ &= \underline{6.858 \cdot 10^5}. \end{aligned}$$

The second approach, due to Atoji (1957), defines the height of the sharpened peak at the origin by

$$P(000) = \int_0^{s_0} 4\pi s^2 \frac{f_j(s) f_k(s)}{(\sum_i f_i / \sum_i z_i)^2} \exp(-\frac{B}{2} s^2) ds$$

where $s = (2 \sin\theta)/\lambda$, s_0 is the maximum value of s , f denotes the scattering factor, and z , the atomic number. By letting $f = \hat{f} \cdot z$ and $B/2 = g$ this expression simplifies to

$$P(000) = \sum_i z_i^2 \int_0^{s_0} 4\pi s^2 \exp(-\frac{B}{2} s^2) ds$$

and is evaluated by letting $\int_0^{s_0} () = \int_0^{\infty} () - \int_{s_0}^{\infty} ()$ where the value of $\int_0^{\infty} ()$ is given in the standard integration tables and $\int_{s_0}^{\infty} ()$ is the Patterson termination error. Consequently

$$\begin{aligned} \int_0^{s_0} () &= \frac{\pi}{g}^{3/2} - \frac{\pi}{g} \sqrt{\frac{\pi}{g}} \operatorname{erfc}(\sqrt{g} \cdot s_0) + 2s_0 \exp(-gs_0^2) \\ &= \frac{\pi}{g}^{3/2} [1 - \operatorname{erfc}(\sqrt{g} \cdot s_0)] - \frac{\pi}{g} \cdot 2s_0 \exp(-gs_0^2) \end{aligned}$$

Since $g = B/2 = 1.36$ and $s_0 = 2/1.542 = 1.30$,

$$\begin{aligned} \int_0^{s_0} () &= 3.51 \operatorname{erf}(1.516) - 6 \exp(-2.3) = 3.51 \cdot 0.968 \\ &\quad - 6 \cdot 0.1 = 2.80 \end{aligned}$$

and

$$P(000) = 2.80 \cdot 48(18^2 + 78^2) = \underline{8.565 \cdot 10^5}.$$

The disagreement between the two results is due chiefly to the fact that the first considers only reflections which were actually recorded whereas the second refers to all

reflections. For the practical purpose of Patterson interpretation, the theoretical height of a sharpened peak is therefore given by

$$P_{\text{theo}}(\text{XYZ}) = \frac{6.86}{8.56} 2.8 z_i z_j = \frac{8}{V} k P_{\text{exp}} + \frac{1}{V} F^2(000)$$

and

$$P_{\text{exp}}(\text{XYZ}) = \frac{1}{250} (2.24 z_i z_j - 6843) = 0.009 z_i z_j - 27.4,$$

where 27.4 is the floor value. Thus experimental peak heights for single Bi-Bi, Bi-Cl, and Cl-Cl vectors are 27.4, -14.8, and -24.5 respectively.

Discovery of large peaks along the P(00Z) line section, indicative of atoms having the same x and y coordinates, gave first experimental proof of the presence of a mirror plane in the c direction. It further established a center of symmetry and confirmed the choice Pnm as the correct space group. Subsequently, Okaya and Pepinsky* reported a negative piezoelectric test for BiCl which does not deny the center of symmetry. The absence of a peak at $\frac{1}{2}, \frac{1}{2}, \frac{1}{2}$ excluded the existence of two-fold and four-fold sets except as listed in Figure 3.

Interpretation of the three-dimensional Patterson proved to be the turning point in the structure determination. All

*Okaya, Y. and Pepinsky, R., Department of Chemistry, Pennsylvania State University, State College, Pennsylvania. Piezoelectric effect of BiCl. Private communication. 1960.

48 Bi positions were located by the same direct approach used for the two-dimensional case. This achievement practically solved the phase problem.

First, a list of all peaks was prepared specifying their position and height. Then, search for eight-fold Bi positions was begun by locating the positions of intraset vectors $0, 0, \pm 2z$ in the $P(XOZ)$ Patterson section shown in Figure 6, thereby establishing the allowed values of the z coordinate. Turning to the $P(X\frac{1}{2}Z)$ section in Figure 7, peaks along the $z = \frac{1}{2}$ edge were taken to represent in part the intraset vectors $\frac{1}{2}\pm 2x, \frac{1}{2}, \frac{1}{2}$ and used to obtain the x coordinates. The matching peaks at $\frac{1}{2}\pm 2x, \frac{1}{2}, \frac{1}{2}\pm 2z$, which are required by eight-fold sets, specified one of the allowed z coordinates. The $P(\frac{1}{2}YZ)$ section shown in Figure 8 served as the source of y coordinates. Here peaks along the $z = \frac{1}{2}$ edge and their counterparts with allowed z values were interpreted to represent the $\frac{1}{2}, \frac{1}{2}\pm 2y, \frac{1}{2}$ and $\frac{1}{2}, \frac{1}{2}\pm 2y, \frac{1}{2}\pm 2z$ intraset vectors, respectively. The intraset screening process was concluded by checking for the presence of $\pm 2x, \pm 2y, 0$ and $\pm 2x, \pm 2y, \pm 2z$ vector peaks corresponding to the proposed combinations.

Search for four-fold sets followed the same general lines although vectors $\frac{1}{2}\pm 2x, \frac{1}{2}, \frac{1}{2}\pm 2z$ and $\frac{1}{2}, \frac{1}{2}\pm 2y, \frac{1}{2}\pm 2z$, and $\pm 2x, \pm 2y, \pm 2z$ were not allowed and the number of checks was reduced accordingly. In all cases, care was taken to observe height requirements corresponding to the multiplicities listed for each

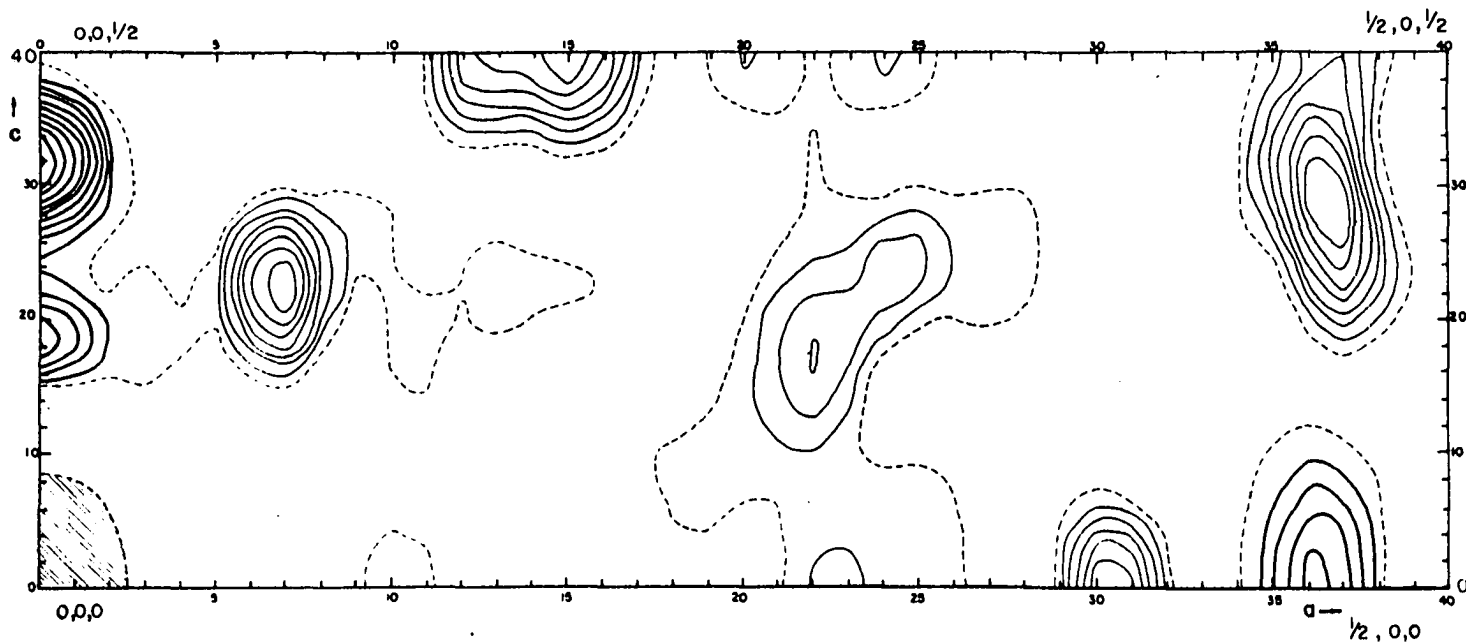


Figure 6. Sharpened Patterson section $P(XOZ)$; thick contours are drawn at intervals corresponding to a Bi-Bi vector, thinner contours represent $2/5$ of this value

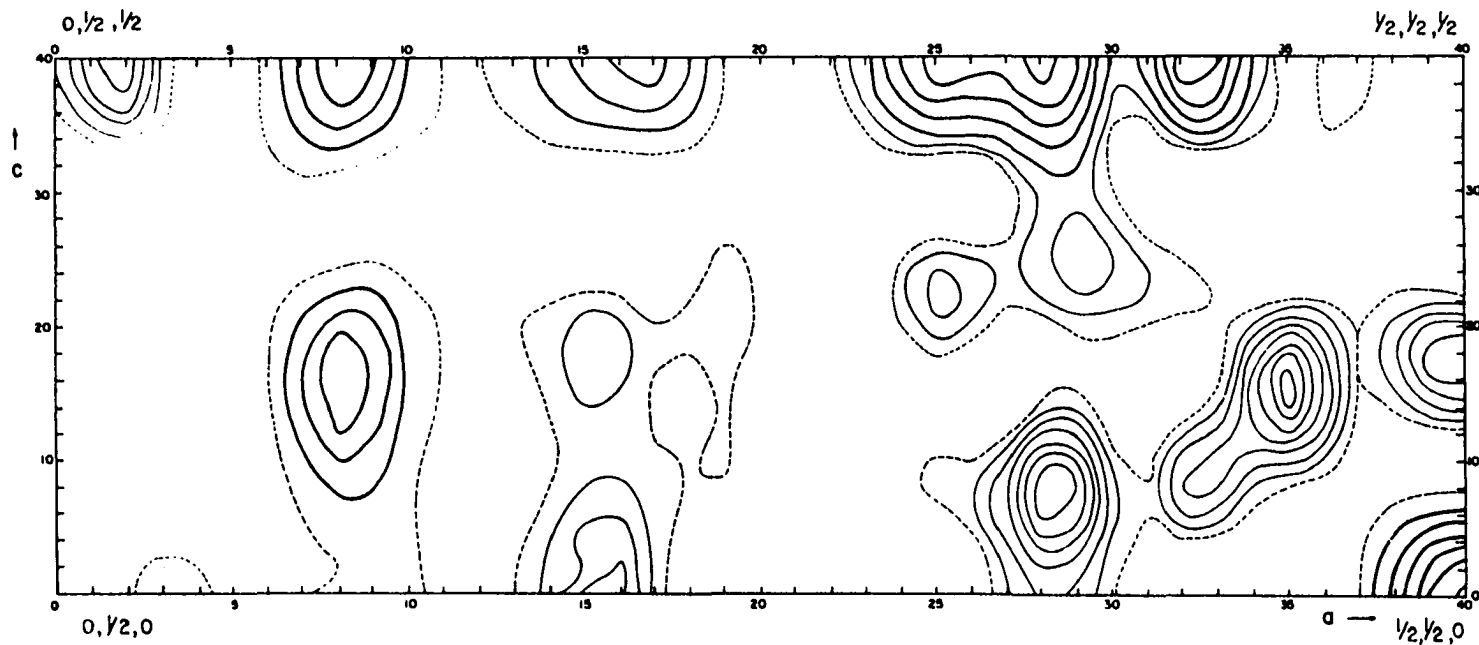


Figure 7. Sharpened Patterson section $P(X_{1/2}Z)$; thick contours are drawn at intervals corresponding to a Bi-Bi vector, thinner contours represent $2/5$ of this value

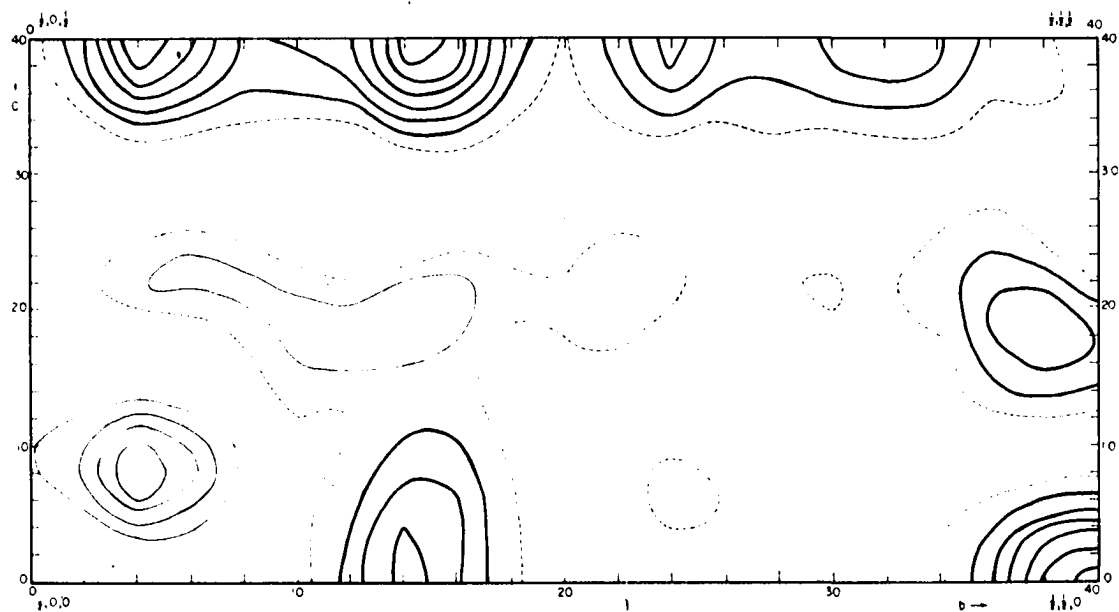


Figure 8. Sharpened Patterson section $P(\frac{1}{2}YZ)$; thick contours are drawn at intervals corresponding to a Bi-Bi vector, thinner contours represent $\frac{2}{5}$ of this value

vector in Table 2.

The characteristic Patterson ambiguity which was touched upon in dealing with the two-dimensional case was now compounded by the two sign possibilities for the z parameter. The choice of origin was again made arbitrarily by selecting a particular representation for one of the eight-fold sets and adopting this as reference for all the other newly-found sets.

In the second stage of interpretation, the Bi positions were further screened by inspection of the respective inter-set vectors which are listed in general form in Table 3. This criterion soon demonstrated its usefulness by proving that one of the three eight-fold Bi positions just acquired was not consistent with the other two. Eventually, two eight-fold and six four-fold sets were located for a total of 40 Bi positions.

The last eight positions played "hard to get" and a special ruse was devised to flush them out. It was reasoned that since there was good evidence for widespread Bi-Bi bonding, at least one atom of the new set or sets would generate a vector about 3 \AA long with the cooperation of one other Bi atom. Close examination of all peaks at the indicated distance from the origin eventually led to the location of the final eight-fold set. All nine independent positions were refined by hand to give the best possible over-all agreement with the position of Patterson peaks. Results are listed in

Table 4.

Calculation of Structure Factors

Structure factors are defined by the general expression:

$$\begin{aligned}
 F(hkl) &= \sum_r f_r(hkl) \exp 2\pi i (hx_r + ky_r + lz_r) \\
 &= \sum_r f_r(hkl) \cos 2\pi(hx_r + ky_r + lz_r) + \\
 &\quad i \sin 2\pi(hx_r + ky_r + lz_r) \\
 &= A' + i B'
 \end{aligned}$$

where f_r is the scattering factor and x_r, y_r, z_r , the coordinates of atom r . Since the structure has a center of symmetry, $F(hkl) = F(\bar{h}\bar{k}\bar{l})$, $A' + iB' = A' - iB'$, $B' = 0$ and the above relation reduces to

$$F(hkl) = \sum_r f_r(hkl) \cos 2\pi(hx_r + ky_r + lz_r)$$

Let $A = \sum_s \cos 2\pi(hx_s + ky_s + lz_s)$ where the summation applies

to equivalent positions in the unit cell only. Then, substituting the general eight-fold positions from Figure 3,

$$\begin{aligned}
 A &= 2 \cos 2\pi(hx + ky + lz) + 2 \cos 2\pi(-hx -ky +lz) \\
 &\quad + 2 \cos 2\pi(hx - ky - lz + \frac{h+k+l}{2}) \\
 &\quad + 2 \cos 2\pi(-hx + ky - lz - \frac{h+k+l}{2})
 \end{aligned}$$

which eventually reduces to

Table 4. Bi positions from Patterson analysis

No. of atom	Positions		
	x	y	z
I	.047	.222	.199
II	.199	.157	.195
III	.412	.457	0
IV	.096	.072	0
V	.071	.399	0
VI	.414	.099	0
VII	.357	.189	$\frac{1}{2}$
VIII	.237	.330	0
IX	.152	.342	.277

$$A = \begin{cases} 8 \cos 2\pi hx \cos 2\pi ky \cos 2\pi lz & \text{for } h + k + l = 2n \\ -8 \sin 2\pi hx \sin 2\pi ky \cos 2\pi lz & \text{for } h + k + l = 2n + 1 \end{cases}$$

for eight-fold sets and half this quantity for four-fold sets. Thus, in its operational form, the structure factor is related to the atomic scattering factors by the equation

$$F(hkl) = \sum_t f_t(hkl) \cdot A_t(hkl) =$$

$$\begin{cases} 8 \sum_t f_t(hkl) \cos 2\pi hx_t \cos 2\pi ky_t \cos 2\pi lz_t & \text{for } h + k + l = 2n \\ -8 \sum_t f_t(hkl) \sin 2\pi hx_t \sin 2\pi ky_t \cos 2\pi lz_t & \text{for } h + k + l = 2n + 1 \end{cases}$$

where the summation applies only to independent atoms in the unit cell.

Atomic scattering factors for Bi^+ and Cl^- were obtained from Ibers*. The Bi^+ factors were based on the Thomas-Fermi-Dirac treatment and came from unpublished work by Thomas, King, and Umeda. The scattering factors for Cl^- were derived by Boys from an earlier paper by Boys and Price.

Before their introduction into structural calculations during the INCOR-IM computation stage, the Bi^+ scattering factors were corrected for anomalous dispersion (Templeton, 1955). Anomalous dispersion of x-ray radiation is due in part to the reduced scattering power of the shielded, inner electrons and, in part, to the interaction of the incident radiation with the characteristic frequency of the scattering electrons. The corrected scattering factor is related to the original scattering factor, f_0 , and to the real and imaginary corrections, $\Delta f'$ and $\Delta f''$ by the equation

$$f = f_0 + \Delta f' + i \Delta f''.$$

Because of the difficulty inherent in handling the imaginary correction it is customary to calculate the absolute magnitude of the corrected scattering factor according to the equation

* Ibers, J. H., Shell Development Company, Emeryville, California. Form factors for Bi, Bi^+ , and Cl^- . Private communication. 1959.

$$f = \sqrt{(f_0 + \Delta f')^2 + (\Delta f'')^2} \cong f_0 + \Delta f' + \frac{1}{2} \frac{(\Delta f'')^2}{f_0 + \Delta f'}$$

The values of $\Delta f'$ and $\Delta f''$ reported by Dauben and Templeton (1955) for Bi atoms and the Cu K α radiation are -5 and 9, respectively. The anomalous dispersion correction was ultimately applied by subtracting 5 from scattering factors at all angles. It was felt that the uncertainty in the charge of the Bi species and the controversy surrounding the anomalous dispersion theory did not warrant the inconvenience of computing the relatively small, second correction term. The correction for Cl atoms is quite negligible and was omitted.

The actual computation of structure factors was performed on the I.B.M. 650 computer using the LS-IIM2 least squares program, and expanded version of LS-II (Senko et al., 1957), which was modified to calculate structure factors only. This modification is designed to reduce the computing time by omitting certain portions of the least squares calculations. Atomic parameters from the three-dimensional Patterson were fed into the program along with the 1938 observed reflections, the scattering factors, the absolute over-all scale factor, and the average temperature factor. The output included observed and calculated structure factors and, for each layer, optimum scale factors, and R_3 residuals. A list of the ob-

served and calculated structure factors for the final structure is given in Appendix B.

Electron Density Maps

With most structure factor signs correctly assigned on the basis of the strongly-diffracting Bi atoms, attention was turned to the computation of electron density maps and the search for Cl positions.

The general expression for the electron density in a crystal is

$$\rho(\text{XYZ}) = \frac{1}{V} \sum_h \sum_k \sum_{l=-\infty}^{\infty} F(hkl) \exp[-2\pi i(hX+hY+lZ)]$$

where X, Y, and Z indicate grid points rather than atomic coordinates. As with the Patterson function, the expression for centrosymmetric structures reduces to

$$\begin{aligned} \rho(\text{XYZ}) &= \frac{8}{V} \sum_h \sum_k \sum_{l=0}^{\infty} F(hkl) \cos 2\pi hX \cos 2\pi kY \cos 2\pi lZ \\ &\quad \text{for } h + k + l = 2n \\ &- \frac{8}{V} \sum_h \sum_k \sum_{l=0}^{\infty} F(hkl) \sin 2\pi hX \sin 2\pi kY \cos 2\pi lZ \\ &\quad \text{for } h + k + l = 2n + 1 \end{aligned}$$

or, more specifically, to

$$\begin{aligned} \rho(\text{XYZ}) &= \frac{1}{V} F(000) + \frac{2}{V} \left[\sum_h F(h00) \cos 2\pi hX + \sum_k F(0k0) \cos 2\pi kY \right. \\ &\quad \left. + \sum_l F(00l) \cos 2\pi lZ \right] + \frac{4}{V} \left[\sum_h \sum_k F(hk0) \cos 2\pi hX \cos 2\pi kY \right. \\ &\quad \left. + \sum_h \sum_l F(h0l) \cos 2\pi hX \cos 2\pi lZ \right] \quad (\text{Continued next page}) \end{aligned}$$

$$\begin{aligned}
& + \sum_h \sum_l F(0kl) \cos 2\pi kY \cos 2\pi lZ] \\
& + \frac{8}{V} \sum_h \sum_k \sum_l F(hkl) \cos 2\pi hX \cos 2\pi kY \cos 2\pi lZ, \text{ for } h+k+l=2n \\
\rho(XYZ) = & - \frac{2}{V} \left[\sum_h F(h00) \sin 2\pi hX + \sum_k F(0k0) \sin 2\pi kY \right. \\
& + \sum_l F(00l) \cos 2\pi lZ] - \frac{4}{V} \left[\sum_h \sum_k F(hk0) \sin 2\pi hX \sin 2\pi kY \right. \\
& + \sum_h \sum_l F(h0l) \sin 2\pi hX \cos 2\pi lZ + \sum_k \sum_l F(0kl) \sin 2\pi kY \\
& \left. \left. \cos 2\pi lZ \right] \right. \\
& - \frac{8}{V} \sum_h \sum_k \sum_l F(hkl) \sin 2\pi hX \sin 2\pi kY \cos 2\pi lZ, \\
& \text{for } h + k + l = 2n + 1
\end{aligned}$$

Structure factors for special reflections were divided by their appropriate multiplicity factors in accordance with the above relations and the summing codes specifying the evenness or oddness of indices and the form of the electron density expression were supplied for each reflection. All unobserved reflections and those with $F_o \gg F_c$ were excluded. The summation was performed on an $1/80 \times 1/80 \times 1/40$ grid with the aid of the I.B.M. 650 computer and the TDF-2 program. Results were again compiled on the I.B.M. 407 tabulator equipped with the special wiring panel. Contours were plotted in the conventional manner. Beside the nine original Bi

positions, 21 other peaks appeared. These are all listed in Table 5.

Table 5. Atomic positions from Fourier analysis

No. of atom	Positions		
	x	y	z
X	0	0	.290
I	.045	.222	.196
	.045	.224	.290
XI	.045	.425	$\frac{1}{2}$
V	.071	.399	0
	.072	.398	.232
IV	.095	.070	0
	.095	.069	.232
XII	.111	.132	$\frac{1}{2}$
XIII	.262	.288	$\frac{1}{2}$
XIV	.290	.054	$\frac{1}{2}$
XV	.314	.017	0
XVI	.334	.210	.192
XVII	.334	.443	.209
	.354	.193	.266
VII	.358	.191	$\frac{1}{2}$
	.380	.272	0
	.409	.459	.232

Interpretation of all 21 peaks as indicative of Cl positions would have resulted in a total of 128 Cl atoms per unit cell in drastic violation of Corbett's chemical analysis. Furthermore, some of the alleged locations were closer to Bi atoms than was allowed by legitimate bond distances. Several devices, including least squares cycles on very limited samples and two-dimensional difference Fourier projections, were used in a vain effort to cope with this excess. Finally, it became evident that more fundamental measures were called for. Some of the extra peaks were thought to have been contributed by reinforced ripples caused by the series termination effects of nearby Bi atoms. A three-dimensional difference Fourier which is free of this defect was expected to save the day.

The difference Fourier, more properly known as the error synthesis, provides a direct portrayal of the discrepancy between the structure represented by the observed intensities and the postulated model. Strongly negative regions in the contour maps indicate that too much scattering matter has been assumed there, while positive regions indicate that too little matter has been assigned. A steep negative gradient at an assumed atomic position implies that the atom is slightly out of place and should be moved toward the nearest positive area. The error synthesis is computed in the same manner as the more conventional Fourier synthesis except that

the signed differences $F_O - F_C$ are used as Fourier coefficients, rather than the observed structure factors with calculated signs.

In order to render the results more meaningful, the original Bi positions and the corresponding temperature factors were partially refined by running 250 reflections, selected more or less at random, through two cycles of the LS-IIM2, least squares program. The results, listed in Table 6, were then used to compute structure factors for the difference Fourier. Contrary to past practice, all operations preliminary to the summation were handled on the I.B.M. 650 computer by means of the new TDF-2 COEFFICIENT program (Stucky, 1960). These operations comprised the elimination of reflections which were unobserved or smaller than a given minimum and reflections with $F_O/F_C > 3$. They also included the division of special reflections by their respective multiplicity factors, the provision of the proper electron density form and summation codes, and the selection of the signed differences $F_O - F_C$ as Fourier coefficients. The summation was carried out in the conventional manner on an $1/80 \times 1/80 \times 1/40$ grid. The output was tabulated and printed directly on a grid-form from which 11 positive and nine negative peaks were read off by inspection. These are reported in Table 7.

The positive peaks, interpreted as Cl positions,

Table 6. Bi parameters refined by LS-IIM2

Atom no.	Position			B	Layer no.	K	R ₃
I	.0463	.2234	.1956	2.02	0	12.68	.0520
II	.1992	.1552	.1870	2.19	1	11.68	.0843
III	.4100	.4570	0	1.44	2	13.74	.0803
IV	.0980	.0698	0	2.08	3	11.50	.0481
V	.0709	.3970	0	2.50	4	10.67	.1173
VI	.4125	.1004	0	2.61	5	12.52	.0579
VII	.3579	.1897	$\frac{1}{2}$	1.58	all		.0657
VIII	.2373	.3284	0	2.01	all (R ₁)		.2442
IX	.1534	.3431	.2710				

Table 7. Atomic positions from three-dimensional difference Fourier

Atom no.	Position			Atom no.	Position		
I	.048	.222	.190	XI	.048	.419	$\frac{1}{2}$
II	.199	.155	.187	XII	.109	.130	$\frac{1}{2}$
III	.411	.456	0	XIII	.261	.286	$\frac{1}{2}$
IV	.099	.071	0	XIV	.291	.054	$\frac{1}{2}$
V	.071	.397	0	XV	.316	.015	0
VI	.414	.102	0	XVI	.334	.216	.191
VII	.357	.194	$\frac{1}{2}$	XVII	.333	.441	.209
VIII	.240	.330	0	XVIII	.433	.329	$\frac{1}{2}$
IX	.152	.341	.269	XIX	.445	.085	.296
X	0	0	.290	XX	.466	.280	0

generated 56 Cl atoms per unit cell, eight more than the number of Bi atoms. These peaks were all part of the group evolved from the three-dimensional Fourier synthesis but their defiance of the 1:1 stoichiometry was less brazen and almost tolerable. The negative peaks were indicative only of anisotropic thermal motion or minor positional shifts for certain Bi atoms.

A drawing of the unit cell, complete with the locations of all atoms found thus far, presented an arrangement which was very plausible, though admittedly unorthodox. Agreement between observed and calculated structure factors was very good for this stage of structure determination and the Bi-Bi vectors checked well with Patterson peaks. It was therefore felt that this model was essentially correct and that the time had come to proclaim victory of mind over matter and to settle down to the lesser tasks of refining the atomic coordinates and temperature factors, calculating interatomic distances and angles, and exercising every legitimate effort to relieve the structure of eight embarrassing Cl atoms.

STRUCTURE REFINEMENT AND FUNCTIONAL ANALYSIS

The process of structure refinement was assigned the dual purpose of pinpointing the atomic coordinates in order that the type of species formed by successive bond ruptures could be identified correctly and of assessing the general accuracy of the proposed model including the eight uncooperative Cl atoms. The functional analysis computation provided bond distances and angles along with their standard deviations.

Refinement of Structure

The structure was refined by the method of least squares. The advantages of this approach lie in the elimination of the series termination error and the provision of a means to regulate the influence of a reflection in such a manner that its contribution be commensurate with the accuracy of the original intensity measurement. The theory of error predicts that, if the errors of observed structure factors follow the Gaussian distribution, then the best atomic parameters will be those which result in the minimization of the residual

$$R = \sum_i [\sqrt{w_i} (|F_o| - |F_c|)_i]^2,$$

where w is a weighting factor. This is the fundamental concept of least squares refinement.

The two programs available for least squares computations

were the LS-IIM2, used previously for calculation of structure factors, and a program by Busing and Levy (1959a) written for the I.B.M. 704 computer. Due to the space and speed limitations of the I.B.M. 650, the LS-IIM2 program solves the system of normal equations on the basis of a diagonal approximation to the full matrix. It was estimated that the Busing and Levy program would be three times more effective and 20 times faster than the "650" program. Five least squares cycles with isotropic temperature factors were run on the I.B.M. 704 computer at the Midwest Universities Research Association in Madison, Wisconsin. The structure refined very satisfactorily lowering the residual

$$R_1 = \frac{\sum \left| |F_o| - |F_c| \right|}{\sum |F_o|}$$

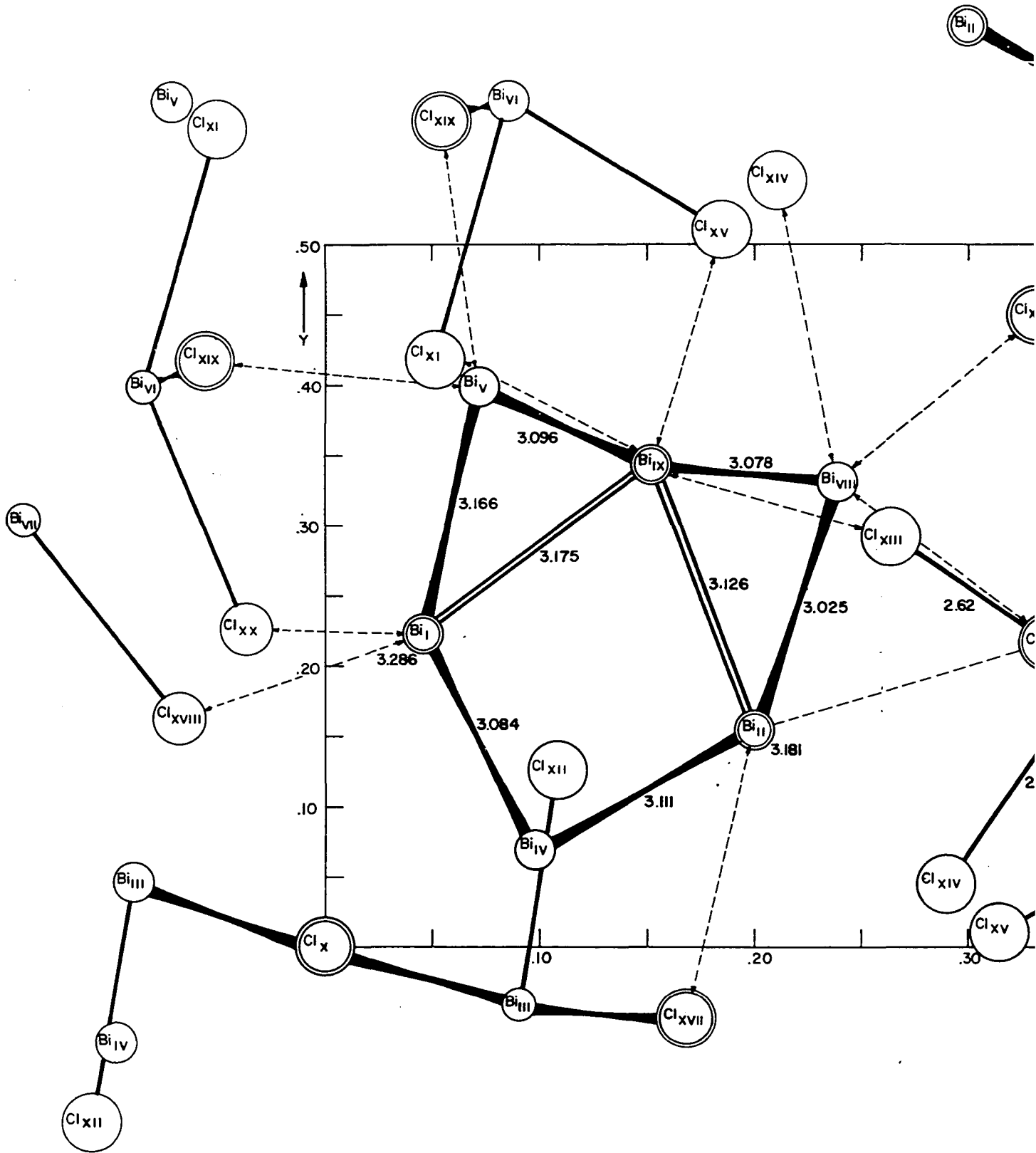
from an initial value of about 0.26 to 0.156. The output of cycle 5 is given in Table 8. Figure 9 shows a drawing of the complete structure, projected on the (001) plane.

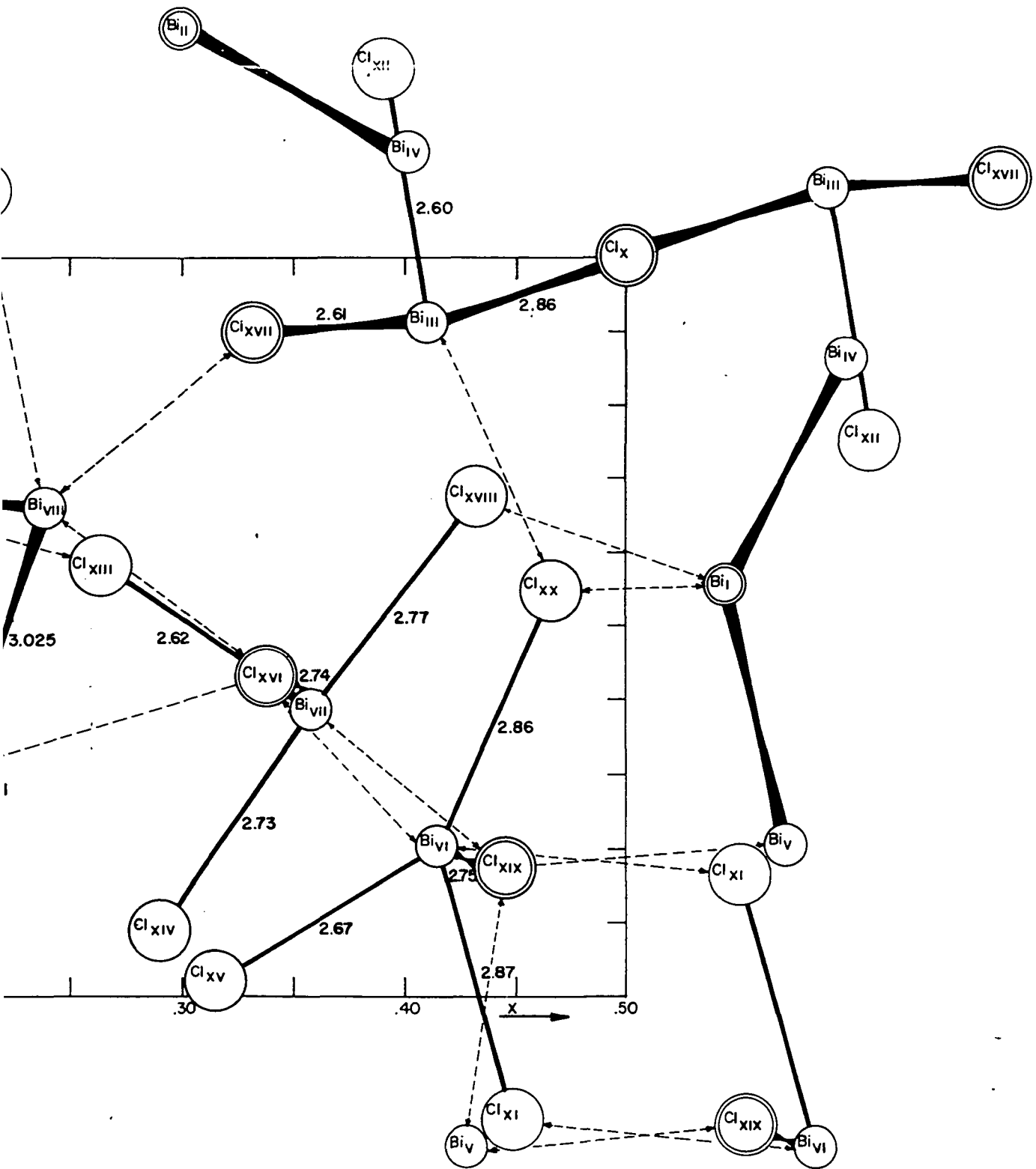
Throughout the refinement no grounds appeared for dismissing any of the Cl positions. As a further check of their validity, a three-dimensional difference Fourier was computed on the basis of the refined parameters following the operational procedure described previously. The lack of negative peaks at the assigned Cl positions confirmed their authenticity and precluded the possibility of disordered Cl atoms.

Table 8. Atomic parameters after final refinement

Atom no.	Positions					B	
I	.0459	\pm .0002	.2229	\pm .0003	.1876	\pm .0007	3.25 \pm .07
II	.2002	\pm .0002	.1544	\pm .0002	.1815	\pm .0006	2.96 \pm .07
III	.4101	\pm .0002	.4550	\pm .0003	0		2.07 \pm .07
IV	.0984	\pm .0002	.0692	\pm .0003	0		2.52 \pm .07
V	.0723	\pm .0003	.3982	\pm .0004	0		3.70 \pm .10
VI	.4139	\pm .0002	.1009	\pm .0004	0		3.39 \pm .10
VII	.3578	\pm .0002	.1930	\pm .0002	$\frac{1}{2}$		1.75 \pm .06
VIII	.2390	\pm .0002	.3296	\pm .0003	0		2.25 \pm .07
IX	.1525	\pm .0002	.3425	\pm .0003	.2669	\pm .0007	3.43 \pm .08
X	0		0		.288	\pm .005	2.3 \pm .4
XI	.052	\pm .001	.418	\pm .002	$\frac{1}{2}$		3.1 \pm .5
XII	.109	\pm .001	.126	\pm .002	$\frac{1}{2}$		2.6 \pm .4
XIII	.264	\pm .002	.291	\pm .003	$\frac{1}{2}$		5.0 \pm .8
XIV	.290	\pm .001	.044	\pm .002	$\frac{1}{2}$		3.6 \pm .5
XV	.315	\pm .001	.010	\pm .002	0		3.5 \pm .5
XVI	.338	\pm .001	.216	\pm .002	.194	\pm .004	3.4 \pm .4
XVII	.332	\pm .001	.449	\pm .002	.216	\pm .004	3.4 \pm .4
XVIII	.433	\pm .001	.337	\pm .001	$\frac{1}{2}$		1.8 \pm .3
XIX	.445	\pm .001	.086	\pm .002	.302	\pm .005	4.5 \pm .5
XX	.466	\pm .001	.274	\pm .001	0		1.2 \pm .3
$K_0 = 12.72,$ $K_2 = 13.50,$ $K_4 = 12.71,$ $R_3 = .187$ $K_1 = 12.00,$ $K_3 = 12.34,$ $K_5 = 13.20,$ $R_1 = .156$							

Figure 9. Structure of BiCl projected onto the (001) plane





Finally, a two-dimensional difference Fourier projection onto the (001) plane, based on the refined Bi parameters alone, produced Cl peaks with the expected height ratios. This served to dispel once again the disorder specter and, even more important, to confirm the presence of eight-fold Cl positions.

The three-dimensional difference Fourier allowed a glance at the anisotropic thermal motion of Bi atoms. Figure 10 shows the positions of anisotropic peaks in relation to Bi atoms. Relative peak heights are given in parentheses; the average height of a Bi peak would be about 450 on the same scale.

Weighting of Intensities

The weighting of individual reflections has been discussed briefly by Lipson and Cochran (1957, pp. 281 and 282). The weighting factor is inversely proportional to the square of an estimated standard deviation of the observed intensity, i.e., $w = 1/\sigma^2(I_o)$. The underlying concept is that the contribution of each reflection to the residual be commensurate with the accuracy assigned to the original observation.

The most valid criterion for the accuracy of an observed intensity is the number of films which contribute to its experimental evaluation. In addition, it is customary to penalize very weak reflections because of their sensitivity

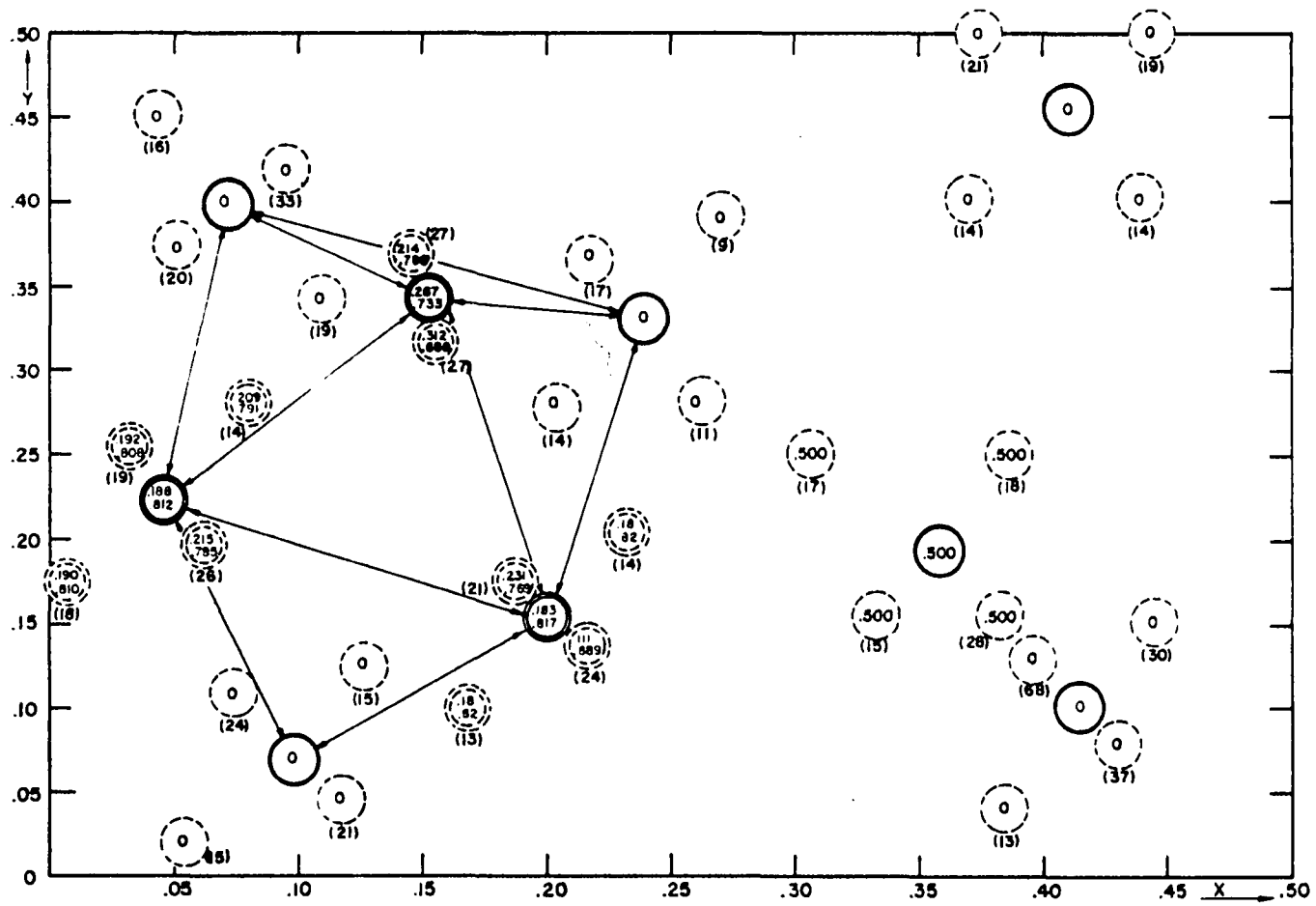


Figure 10. Anisotropic thermal motion of Bi atoms

to minute variations in the film background. For each set of Weissenberg intensities there exists a quantity I_m , the lowest observable intensity, and a quantity I_b , the midpoint of the best judged range. I_b is often equal to 16 I_m .

Reflections with $I_o \geq I_b$ fell generally within the judgeable range on the maximum number of films (3). Their relative error was therefore assumed constant and estimated at 10% on the basis of the observed precision. Mathematically this condition is expressed by

$$\frac{\sigma(I_o)}{I_o} = 0.1$$

For reflections with $I_o < I_b$, the relative error should rise gently at first for decreasing intensities, as the number of contributing films drops to two, then, more rapidly, as only one film becomes available and background variations gain in importance. The relation

$$\frac{\sigma(I_o)}{I_o} = 0.1 \left(\frac{I_b}{I_o} \right)^{3/4}$$

was found to satisfy the statistical formula for the change in standard deviation with decreasing number of observations and to coincide with a reasonable estimate for the error of I_m .

The contribution of errors in the Lorentz, polarization, and absorption corrections to the standard deviations of corrected intensities was calculated by means of the formula for the propagation of error. If

$$I_{\text{corr}} = I_{\text{uncorr}} \cdot \chi_{\text{LPA}},$$

where χ_{LPA} is the product of the Lorentz, polarization, and absorption correction, then

$$\begin{aligned} (\sigma_{I_{corr}}) &= \left\{ \sigma^2(\chi) \left[\frac{\partial(I_{corr})}{\partial\chi} \right]^2 + \sigma^2(I_{uncorr}) \left[\frac{\partial(I_{corr})}{\partial(I_{uncorr})} \right]^2 \right\}^{\frac{1}{2}} \\ &= \left\{ \sigma^2(\chi) I_{uncorr}^2 + \sigma^2(I_{uncorr}) \cdot \chi^2 \right\}^{\frac{1}{2}} \end{aligned}$$

Assuming only experimental error and neglecting any inaccuracies inherent in the theoretical treatment of these corrections, it was found that

$$\left[\frac{\sigma(\chi)}{\chi} \right]^2 \ll \left[\frac{\sigma(I_{uncorr})}{I_{uncorr}} \right]^2$$

This reduced the above expression to

$$\sigma(I_{corr}) \cong \sigma(I_{uncorr}) \cdot \chi$$

or

$$\frac{\sigma(I_{corr})}{I_{corr}} \cong \frac{\sigma(I_{uncorr})}{I_{corr}} \cdot \chi = \frac{\sigma(I_{uncorr})}{I_{uncorr}}$$

The Busing and Levy least squares program requires for each reflection the standard deviation of the structure factor. It can be shown that this quantity is related to the standard deviation of the observed intensity by the equation

$$\sigma(F_o) = \frac{1}{2} \frac{\sigma(I_{corr})}{I_{corr}} F_o \cong \frac{1}{2} \frac{\sigma(I_o)}{I_o} F_o$$

Substituting in the earlier expressions for $\sigma(I_o)$, the working formulation of $\sigma(F_o)$ becomes

$$\sigma(F_o) = \begin{cases} .05 F_o & \text{for } I_o \geq I_b \\ .05 \left(\frac{I_b}{I_o} \right)^{3/4} F_o & \text{for } I_o < I_b \end{cases}$$

A new program, identified as "STD", was written for the I.B.M. 650 computer for the purpose of computing standard deviations of structure factors on the basis of uncorrected intensities. A detailed writeup will be found in Appendix A.

Figure 11 compares a graphic representation of this treatment with corresponding plots based on a scheme by Williams and Fitzwater as incorporated in the LS-IIM2 program. The major faults of the latter approach lie in its failure to base calculation of standard deviations on the uncorrected intensities and in the inordinately sharp rise of $\sigma(F_o)$ for weak reflections. This causes incorrect assignment of error estimates and the virtual elimination of contributions from very weak reflections.

Neither treatment considered the weighting of unobserved reflections. A detailed discussion of this problem has been presented by Hamilton (1955).

Functional Analysis

Interatomic distances and angles, along with their respective standard deviations, were computed by Dr. Lawrence Dahl at M.U.R.A. with the aid of the Crystallographic Function and Error program (Busing and Levy, 1959b). These are listed in Tables 9 and 10. Bonding distances are indicated in Figure 9.

Table 9. Interatomic distances in Å

Atom No.	Distance	Atom No.	Distance
I-I	3.286 ± .012	VII-XIII	2.617 ± .050
I-II	3.704 ± .005	VII-XIV	2.730 ± .034
I-IV	3.084 ± .006	VII-XVI	2.743 ± .037
I-V	3.166 ± .007	VII-XVIII	2.775 ± .021
I-IX	3.125 ± .006	VII-XIX	3.100 ± .037
I-X	3.625 ± .011	VIII-IX	3.078 ± .006
I-XII	3.424 ± .017	VIII-XIV	3.296 ± .034
I-XVIII	3.215 ± .018	VIII-XVI	3.311 ± .029
I-XIX	3.700 ± .032	VIII-XVII	3.378 ± .028
I-XX	3.297 ± .011		
II-II	3.181 ± .011	IX-XI	3.297 ± .024
II-IV	3.111 ± .006	IX-XII	3.977 ± .023
II-VIII	3.205 ± .005	IX-XIII	3.373 ± .040
II-IX	3.126 ± .006		
II-XII	3.525 ± .017	X-XII	3.64 ± .03
II-XIII	3.763 ± .034	X-XVII	3.94 ± .02
II-XIV	3.850 ± .024	X-XVIII	3.84 ± .03
II-XV	3.771 ± .031	X-XX	3.95 ± .02
II-XVI	3.305 ± .025		
II-XVII	3.306 ± .025	XI-XI	3.43 ± .06
III-X	2.860 ± .028	XI-XV	3.38 ± .05
III-XII	2.605 ± .027	XI-XIX	3.62 ± .05
III-XVII	2.606 ± .032	XI-XIX	3.67 ± .05
III-XX	3.017 ± .018	XI-XX	3.48 ± .03
IV-X	3.553 ± .030		
IV-XVII	3.470 ± .031	XII-XVII	3.54 ± .04
IV-XVIII	3.557 ± .021	XII-XX	3.61 ± .03
V-VIII	3.979 ± .007		
V-IX	3.096 ± .007	XIII-XIV	3.76 ± .06
V-XIV	3.859 ± .035	XIII-XVI	3.36 ± .05
V-XIX	3.418 ± .037	XIII-XVII	3.79 ± .05
V-XIX	3.337 ± .036	XIII-XVIII	3.95 ± .05
VI-XI	3.185 ± .031	XIV-XVI	3.89 ± .04
VI-XI	2.870 ± .031	XIV-XVII	3.68 ± .04
VI-XV	2.666 ± .035	XV-XVI	3.58 ± .04
VI-XVI	3.000 ± .030		
VI-XIX	2.753 ± .046	XVI-XVI	3.40 ± .08
VI-XX	2.865 ± .018	XVI-XVII	3.50 ± .03
		XVI-XVIII	3.91 ± .03
		XVI-XIX	3.29 ± .04
		XVI-XX	3.53 ± .03

Table 9. (Continued)

Atom No.	Distance	Atom No.	Distance
XVII-XVII	3.78 ± .07	XIX-XIX	3.46 ± .09
XVII-XVIII	3.79 ± .03	XIX-XIX	3.63 ± .06
		XIX-XX	3.90 ± .04

Table 10. Interatomic angles; central atom is vertex

Atom No.	Angle	Atom No.	Angle
I - I -V	58.7 ± .1	XV-VI -XX	145.8 ± .9
II - I -V	92.3 ± .2	XIX-VI -XIX	148.5 ± 1.4
I -II -VIII	92.7 ± .1	XIII-VII-XIV	89.3 ± 1.3
X -III-X	80.7 ± 1.3	XIII-VII-XVI	77.7 ± .6
X -III-XII	83.5 ± .5	XIII-VII-XVIII	94.2 ± 1.2
X -III-XVII	92.2 ± .9	XIV-VII-XVIII	176.5 ± .8
XII-III-XVII	85.4 ± .7	XVI-VII-XVI	155.4 ± 1.1
XVII-III-XVII	92.8 ± 1.3	II-VIII-V	86.8 ± .1
I -IV -II	73.4 ± .1	I-IV -VIII	107.7 ± .2
I -IV -II	105.1 ± .2	II-IX -V	105.9 ± .2
I -V -I	37.9 ± .1	V-IX -VIII	80.2 ± .2
I -V -VIII	88.3 ± .2	XVI-XIV-XVI	87.2 ± 1.2
XI -VI -XV	75.2 ± 1.0	XIV-XVI-XVIII	89.8 ± .9
XI -VI -XIX	81.4 ± .7	XVI-XVIII-XVI	86.5 ± 1.0
XI -VI -XX	139.0 ± .7		

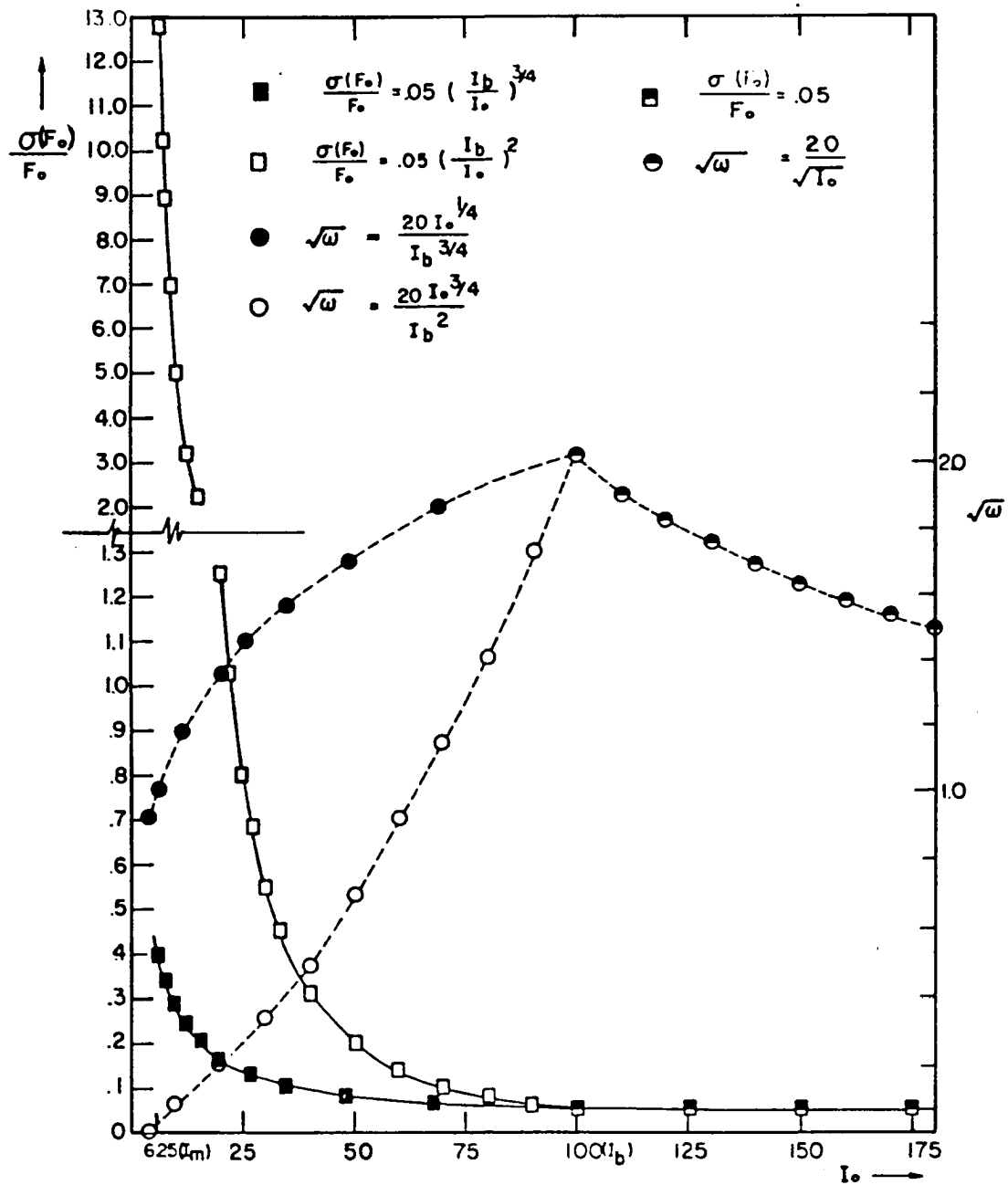


Figure 11. Standard deviation plots; full circles indicate the new approach

DISCUSSION

Interpretation of Structure

The unit cell of bismuth monochloride contains four Bi_9 polyhedra and an array of Bi and Cl atoms which can be catalogued as eight BiCl_5 and two Bi_2Cl_8 units. The Bi_9 polyhedron assumes the form of a distorted trigonal prism with atoms Bi_{IV} and Bi_{IX} (2) projecting from its faces. In BiCl_5 the Cl atoms form a distorted tetragonal pyramid about Bi; in Bi_2Cl_8 two such pyramids share an edge. Weak Bi-Cl interactions form the only links between molecules. Those shorter than 3.5 \AA are indicated by dashed lines in Figure 9.

Each atom in the Bi_9 unit has four nearest neighbors at 3.08 \AA to 3.29 \AA . The shorter distance is the same as that between Bi and its three nearest neighbors in solid bismuth, the longer is comparable to the 3.32 \AA distance in liquid bismuth. The elongation of Bi-Bi bonds and the concomitant distortion of the trigonal prism is induced by intermolecular Bi-Cl interactions whose average length of 3.3 \AA is very close to the sum of the estimated Bi^+ and Cl^- ionic radii.

The effective radius, r , of an atom in a crystal lattice can be calculated by Pauling's (Pauling and Pauling, 1956) formula

$$r = r_1 - 0.300 \log_{10} \frac{v}{n}$$

from its simple covalent radius, r_1 , its valence, v , and the

number of bonds it forms, n . For a Bi atom bonded to four neighbors, $r_1 = 1.510$, $n = 4$ and the simplified expression becomes

$$r = 1.510 - 0.300 \log_{10} \frac{v}{4} .$$

On this basis, a valence of 2 corresponds to an effective bond length of 3.20 Å, a valence of 3, to 3.09 Å, and a valence of 4, to the single covalent bond length of 3.02 Å. Since the distortion of the trigonal prism involves considerable stretching of most bonds and only slight compression of a few, the valence of 2 is incompatible with the average experimental bond length of 3.14 Å. The two other values are acceptable at this stage as they call for bonds which are either equal to or smaller than the shortest experimental distance, 3.08 Å.

The valence of 3 would place no charge on the Bi atom; the three bonding p electrons could distribute themselves among four metallic orbitals, each equivalent to 3/4 of an atomic orbital in accordance with Pauling's findings, and an inert s pair would be left to take up the void opposite from the center of the Bi₉ unit. However, such a disposition is incompatible with the diamagnetic character of the crystals as it calls for an odd number of electrons in the polyhedron. The valence of 4 requires a +1 charge on each Bi atom and, presumably, entails the distribution of two s and two p electrons among four highly distorted sp³ orbitals. The happiest solution, however, stems from a molecular orbital approach

which can justify an intermediate valence and hence an intermediate net charge. Under these circumstances the pyramidal molecules can be regarded as BiCl_5^- and Bi_2Cl_8^- ions containing bismuth in its conventional Bi(III) state and Bi_9 is assigned a charge of +5 to insure charge conservation.

Bi-Cl bond lengths within the pyramidal molecules range between 2.60 and 2.87 Å. They are comparable to the Bi-Cl distance of 2.71 Å in BiSCl and BiSeCl but longer than the 2.48 Å distance in gaseous BiCl_3 . Calculations based on the electronegativities of the two elements assign 25% ionic character to the Bi-Cl bond, but the distance in gaseous BiCl_3 is equal to the sum of covalent radii. The most perplexing aspect of bonding in the BiCl_5^- and Bi_2Cl_8^- ions is the role of the bridging intermolecular links between their Bi and Cl atoms which in this case are only 3.1 Å long. If these are counted along with the regular Bi-Cl bonds, atoms Bi_{III} , Bi_{VI} , and Bi_{VII} attain a sixfold, sevenfold, and even eightfold coordination. Bonds within the pyramidal ions are considered essentially covalent with some ionic character present. Their stretching is due to the intermolecular interactions but also to packing interference and, in the case of the Bi_2Cl_8^- ion, to the sharing of Cl atoms.

Reliability of Model

The consistency of Bi-Bi vectors with the observed Patterson peaks, the agreement between observed and calculated

structure factors, the satisfactory progress of refinement, and the plausibility of the resulting configurations and interatomic distances all serve to insure that the proposed model is essentially correct. The residual

$$R_1 = \frac{\sum \left| |F_o| - |F_c| \right|}{\sum |F_o|},$$

expressing the degree of agreement between observed and calculated structure factors, is most commonly quoted as a measure of accuracy of a model because it is more amenable to numerical treatment than the other criteria. This residual gives a good indication of the progress of refinement but does not in itself constitute an adequate measure of the correctness of a model since all reflections, weak or strong, are assigned equal weight.

According to Lipson and Cochran (1957, p. 147), the only valid basis for the assessment of the correctness (as distinct from accuracy) of a structure lies in the agreement for individual reflections. For reflections which are reasonably strong, and thus reliably estimated, the observed and calculated structure factors should agree to within 40%, most of them being much better than this. A survey of the 55 strongest reflections showed that their structure factors, on the average, agreed within 11% and only two showed a discrepancy higher than 20%.

Several factors must be borne in mind when considering

the 15.6% value of the unweighted residual R_1 calculated by the least squares program. On the negative side of the ledger, this figure takes no account of unobserved reflections. In general, weak reflections showed poorer agreement, as indicated by the slightly higher value (18.7%) of the weighted residual R_3 , so that the inclusion of unobserved reflections should be expected to increase R_1 somewhat. The implication of this fact, borne out by an inspection of positional standard deviations in Table 8, is that the stronger diffracting Bi atoms have been located more reliably than the Cl atoms.

The extenuating circumstances, on the other hand, are more numerous and more consequential. The residual was computed by forcing isotropic temperature factors on the refinement process although Figure 10 indicates considerable thermal anisotropy for Bi atoms. The absorption correction factors differed by as much as 5,000% between reflections, and a slight error in the correction curve would carry very serious consequences. Finally, no allowance was made for secondary extinction simply because no handy correction scheme is yet available. This effect is brought on by the reduction of the intensity of the primary beam incident upon a plane due to reflection from the preceding planes and is expected to be quite important for a crystal containing strongly diffracting bismuth.

Although some doubt remains as to the exact location of

the Cl atoms, special precautions, described in the refinement section, were taken to verify their number. In addition, the density of 6.56 g/cc calculated for 48 Bi and 56 Cl atoms compares much better with the 6.54 g/cc experimental value than the 6.41 g/cc figure calculated on the basis of 48 Bi and 48 Cl atoms per unit cell.

Conclusions

The establishment of atomic configuration in solid BiCl provides a foundation upon which a framework of speculation can be constructed concerning the nature of species formed when bismuth metal or BiCl is dissolved in liquid BiCl₃. As the vigor of disruptive forces induced by thermal motion increases with rising temperature, a process of structural breakdown and interaction of the fragments with the BiCl₃ solvent can be envisioned. At the melting point the intermolecular interactions are destroyed and the crystal structure collapses. There is partial disproportionation of Bi₉⁺⁵ to Bi metal and Bi⁺³ ions and partial dissociation of BiCl₅⁼ and Bi₂Cl₈⁼. The metal-rich liquid phase contains Bi₉⁺⁵ and Cl⁻ ions dissolved in the metal, the salt-rich phase is composed of Bi₉⁺⁵ cations and Cl⁻, BiCl₄⁻, and BiCl₅⁼ anions in equilibrium with BiCl₃. At higher temperatures, nearly complete breakdown of all molecular species takes place to produce a single liquid phase composed of Bi⁺⁵ and Cl⁻ ions along with

solvated metallic electrons.

The presence of all these species in Bi-BiCl₃ solutions, with the exception of Bi₉⁺⁵, had been conjectured by researchers at one time or another. Topol et al. (1960) proposed the formation of BiCl₄⁻ and BiCl₅⁼ ions to account for the high cryoscopic number of alkali chlorides dissolved in molten BiCl₃ after detecting K₃BiCl₆ and K₂BiCl₅ in the KCl-BiCl₃ phase diagram. Subsequent spectroscopic work by Boston and Smith (1960) and concentration cell e.m.f. measurements of Topol et al. (1961) indicated the presence of simple species such as BiCl and (BiCl)₃ in very dilute solutions or at elevated temperatures and the formation of unidentified polymers at increased concentrations. The presence of Bi₉⁺⁵ polymers accounts for the high viscosity of the salt-rich phase while the complexity of the BiCl structure explains the marked tendency of concentrated solutions toward supercooling.

From the vantage point of an archeologist who dug for an earthen vase but ends up surveying an ancient hamlet which he has freed from its burden of overlying sand and debris, it becomes apparent that the finished product has outgrown the original scope of the investigation. What was to be a physical tool for prying into chemical secrets became an achievement which stands on its own merits, opens up a Pandora's box of exciting fact and speculation, and echoes the words of Clarence R. Wylie:

". . . Bridges stand, and men no longer crawl
In two dimensions. And such triumphs stem
In no small measure from the power this game,
Played with thrice-attenuated shades
Of things, has over their originals.
How frail the wand, but how profound the spell!"

SUMMARY

Bismuth monochloride separates out as a solid phase when bismuth metal is dissolved in liquid BiCl_3 . Its crystals take the form of black diamagnetic needles with a flattened hexagonal cross section. The crystal structure of bismuth monochloride was determined as an aid in the identification of the species formed in the Bi- BiCl_3 system.

The stoichiometric formula of bismuth monochloride was found to be $\text{BiCl}_{1.17}$. The crystals are orthorhombic with lattice constants $a_0 = 23.057$, $b_0 = 15.040 \text{ \AA}$, $c_0 = 8.761 \text{ \AA}$ and space group Pnm. The experimental density of 6.54 g/cc agrees well with the 6.56 g/cc value calculated on the basis of the 48 Bi and 56 Cl atoms per unit cell. Three-dimensional Weissenberg and precession film data were obtained with Cu K α radiation. The 2500 reflections were judged visually, and corrected for the Lorentz factor, polarization, absorption, and multiplicity.

The structure was determined by the heavy atom technique. Interpretation of a three-dimensional Patterson map located all 48 Bi positions and thus established the phases of the more important reflections. The 56 Cl positions were found through three-dimensional Fourier and difference Fourier maps. Refinement of the structure was carried out by the least squares technique using isotropic temperature factors. All positions refined satisfactorily resulting in a final R_1

value of 0.156.

Each unit cell contains four Bi_9^{+5} cations in the shape of distorted trigonal prisms that have a Bi atom projecting from each face. There are also eight BiCl_5^- and two Bi_2Cl_8^- anions where the Cl atoms assume a distorted tetragonal pyramidal configuration about Bi. The cation has delocalized bonding and a charge of +5 based on the assignment of Bi(III) atoms to the anions. The latter are thought to have conventional Bi-Cl bonds. Intermolecular linkage is provided by weak Bi-Cl interactions which are considerably shorter between anions than between an anion and the cation. They are responsible for the configurational distortions. A mode of structural breakdown with rising temperature is proposed and the species formed by interaction of the fragments with the BiCl_3 solvent are compared with results of previous investigations.

LITERATURE CITED

- Atoji, M. 1957. *Acta Cryst.* 10, 291.
- Bond, W. L. 1951. *Rev. Sci. Instr.* 22, 344.
- _____. 1959. *Acta Cryst.* 12, 375.
- Boston, C. R. and Smith, G. P. 1960. U. S. Atomic Energy Commission Report ORNL 2988, 9 [Oak Ridge National Lab., Tennessee].
- Bradley, A. J. 1935. *Proc. Phys. Soc.* 47, 879.
- Bredig, M. A. 1959. *J. Phys. Chem.* 63, 978.
- Buerger, M. J. 1942. *X-ray Crystallography*. J. Wiley and Sons, New York.
- _____. 1960. *Crystal Structure Analysis*. J. Wiley and Sons, New York.
- Busing, W. R. and Levy, H. A. 1959a. U. S. Atomic Energy Commission Report ORNL 59-4-37 [Oak Ridge National Lab., Tennessee].
- _____ and _____. 1959b. *Ibid.* ORNL-59-12-3.
- Corbett, J. D. 1958. *J. Am. Chem. Soc.* 80, 4757.
- _____. 1961. *The Solution of Metals in Their Molten Salts*. In Sundheim, B. R. and Gruen, D. M., eds. *Molten Salts*. McGraw-Hill, New York.
- _____, von Winbush, S., and Albers, F. C. 1957. *J. Am. Chem. Soc.* 79, 3020.
- Cubicciotti, D. 1952. *J. Am. Chem. Soc.* 74, 1198.
- _____. 1960a. *J. Chem. Educ.* 37, 540.
- _____. 1960b. *J. Phys. Chem.* 64, 791.
- _____, Keneshea, F. J., Jr., and Kelley, C. M. 1958. *J. Phys. Chem.* 62, 463.
- Darnell, A. J. and Yosim, S. J. 1959. *J. Phys. Chem.* 63, 1813.

- Dauben, C. H. and Templeton, D. H. 1955. Acta Cryst. 8, 841.
- Donges, E. 1950. Z. anorg. Chem. 263, 112, 280.
- Eggink, B. G. 1908. Z. physik. Chem. 64, 449.
- Fitzwater, D. R. 1958. Structures of Some Hydrated Rare Earth Ethylsulfates. Unpublished Ph. D. Thesis. Library, Iowa State University of Science and Technology, Ames, Iowa.
- _____ and Williams, D. E. 1959. The TDF-2, Three-dimensional Fourier Program. (Mimeographed) Department of Chemistry, Iowa State University of Science and Technology, Ames, Iowa.
- Hamilton, W. C. 1955. Acta Cryst. 8, 185.
- Holecek, O. C. 1953. Physical-Chemical Investigation of the System Bi-BiCl₃. Unpublished M. S. Thesis. Library, University of Southern California, Los Angeles, Cal.
- Jones, M. and Lapworth, A. 1914. J. Chem. Soc. 105, 1804.
- Keneshea, F. J., Jr., and Cubicciotti, D. 1958. J. Phys. Chem. 62, 843.
- Levy, H. A., Bredig, M. A., Danford, M. D., and Agron, P. A. 1960. J. Phys. Chem. 64, 1959.
- Lipson, H. and Cochran, W. 1957. The Determination of Crystal Structures. G. Bell and Sons, London.
- Mayer, S. W., Yosim, S. J., and Topol, L. E. 1960. J. Phys. Chem. 64, 238.
- Patterson, A. L. 1935. Z. Krist. 90, 517.
- Pauling, L. and Pauling P. 1956. Acta Cryst. 9, 127.
- Senko, M. E. and Templeton, D. H. 1957. The LS-II, Least Squares Program. (Mimeographed) Department of Chemistry, University of California, Berkeley, Cal.
- Sillen, L. G. and Edstrand, M. 1942. Z. Krist. 104, 178.
- Skinner, H. A. and Sutton, L. E. 1940. Trans. Far. Soc. 36, 681.

- Sokolova, M. A., Urazov, G. G., and Kuznetsov, V. G. 1954. Khim. Redkikh Elementov 1, 102.
- Sokolova, T. I. 1952. Izvest. Sektora Fiz.-Khim. Anal. 21, 159. [U. S. Atomic Energy Commission Translation No. 3168].
- Stucky, G. D. and Fitzwater, D. R. 1960. The TDF-2 COEFFICIENT Program. (Mimeographed) Department of Chemistry, Iowa State University of Science and Technology, Ames, Iowa.
- Templeton, D. H. 1955. Acta Cryst. 8, 842.
- Topol, L. E., Mayer, S. W., and Ransom, L. D. 1960. J. Phys. Chem. 64, 862.
- _____, Yosim, S. J., and Osteryoung, R. A. 1961. [To be published in J. Phys. Chem. ca. 1961.]
- Wilson, A. J. C. 1942. Nature 150, 152.
- Wolten, G. M. and Mayer, S. W. 1958. Acta Cryst. 11, 739.
- Yosim, S. J., Darnell, A. J., W. G. Gehman, and Mayer, S. W. 1959. J. Phys. Chem. 63, 230.
- Zalkin, A. and Jones, R. E. 1957. The INCOR-I, Intensity Correction Program. (Mimeographed) Department of Chemistry, University of California, Berkeley, Cal.

ACKNOWLEDGEMENTS

The successful completion of this project constituted a hardy initiation into the complex field of crystallography, especially for a neophyte lacking the benefit of ready access to an organic source of technical information. In fact, the entire venture would today have been but a bad memory were it not for the generosity and inspiration of my mentor and friend, John Corbett. Time after time his keen intuition shattered the barriers of experimental adversities while his trust and gentle manner restored the self-confidence needed to raise me from occasional depths of dejection. I am deeply grateful for having had the privilege of associating with the man whom I admire as a scientist and value as an individual.

For my crystallographic training I am greatly indebted to Masao Atoji whose prodigious command of the subject, painstaking preparation of lectures, and cordial desire to help will long be remembered.

In the last year I came to rely more heavily on Don Williams for clarification of crystallographic mysteries. His willingness to share with me facts and ideas, sometimes grudgingly but always with enviable competence and thoroughness, have earned him my sincere appreciation.

From Bob Fitzwater came much discouragement and adverse criticism but also a great deal of valuable information,

particularly in the computing field. His general assistance and his generosity in connection with the trip to the 1958 A.C.A. convention are gratefully acknowledged.

During the necessarily brief span of professional association with Larry Dahl I have benefited greatly from his advice, interest, and physical assistance. He has earned the esteem and gratitude of all who knew him and I consider myself fortunate to be in that number.

I am indebted to Professor Rundle for the use of crystallographic equipment and for his guidance through the initial stages of this work.

The high standards demanded of the experimental data by the complexity of this structure were met through the keenness and patience of Pat Hutcheson who was charged with the unenviable task of evaluating diffraction intensities.

Finally, I wish to express my sincere gratitude to my many friends and associates at the Ames Laboratory for their stimulating discussions, gracious assistance, and gratifying companionship.

APPENDIX A: COMPUTER PROGRAMS

Absorption Correction and Sharpening Program

Introduction

This program applies spherical or cylindrical absorption corrections to observed Weissenberg intensities and structure factors and/or multiplies intensities by an optional sharpening factor. A provision is included for multiplying intensities and structure factors by a constant during either operation.

Description of input cards

Absorption correction deck (15 cards)

/ $A^*(10)$, PP/ in fields 1-7.

A^* is the absorption correction at .01 increments of $\sin^2\theta$, as described in the discussion section. PP = 50 + p, where p is the power of 10 multiplying $A^*(10)$.

These cards must be left out if absorption correction is not desired.

Constant cards

/ $\cos^2\nu$ (10), PP/ $\cos\nu$ (10), PP / K_a (10), PP/

ν is defined in the discussion section, K_a is a constant which multiplies the absorption-corrected intensities. This card must be left out if absorption correc-

tion is not desired.

$/\pm B'/\lambda^2(10), PP/\sum_i Z_i \cdot 10^6(10), PP/n_1(10), PP/n_2(10), PP/$

$/n_3(10), PP/n_4(10), PP/K_S(10), PP/$

$\pm B'/\lambda^2$ is the artificial temperature factor defined in the discussion section, $\sum_i Z_i$ is the sum of atomic numbers for all atoms in the unit cell, n_i is the number of atoms of the i -th type in the unit cell (in the same order as the scattering factors), K_S is a constant which multiplies the sharpened intensities and sets $K_a = 1$ if both are included. This card must be left out if sharpening is not desired.

Data cards

$/hhkkllaaaa/I_0(7)/\sin^2\theta(10)/f_1(6)/f_2(6)/f_3(6)/f_4(6)/$

$aaaa = \text{anything}, I_0$ is the unprocessed intensity, f_i is the scattering factor for the atom of type i . These cards have the same format as the INCOR-IM output cards.

Operating instructions

Loading sequence

1. ACS Program deck
2. Switch card
3. Absorption Correction deck (optional)
4. Control cards #1 and/or #2
5. Data cards

Console settings

Storage entry: 70 1952 9999 (00 0000 1999 if program loaded)

Programmed:	STOP	Display:	PROGRAM
Half cycle:	RUN	Overflow:	SENSE
Control:	RUN	Error:	STOP

Operation

Use FORTRANSIT OBJECT wiring panel.

A machine stop with 0050 or 0051 in address lights indicates error in the format of absorption correction or constant cards.

Computation times are 2.1 sec. per reflection for absorption correction and 2.3 sec. per reflection for the sharpening operation.

Description of output cards

/hhkkllaaaa/I_c(7), F₀(2)/sin²θ(10)/f₁(6)/ etc.

I_c is the absorption corrected and/or sharpened intensity. These output cards are in the proper format for input to the LS-IIM2 least squares program.

Discussion

Absorption corrections are calculated according to the method developed by Bond (1959). The correction factor A*, defined as the ratio of the corrected to the observed

intensity, is listed in Bond's paper as a function of μR and $\sin^2\theta$. μ is the linear absorption coefficient and R is defined by the relation

$$R = R_0 \sec \nu$$

where R_0 is the radius of the crystal cylinder and ν is the angle between the incident x-ray beam and a plane normal to the cylinder axis. For spherical crystals and for zero layer photographs of cylindrical crystals $\nu = 0$, $\sec \nu = 1$, and $R = R_0$.

For higher layer reflections, the absorption correction factor undergoes the transition

$$A^*(\mu R_0, \theta) \rightarrow \cos \nu \cdot A^*(\mu R, \tau/2).$$

τ is related to ν and θ by the expression

$$\cos \frac{\tau}{2} = \frac{\cos \theta}{\cos \nu} \quad \text{or} \quad \sin^2 \frac{\tau}{2} = 1 - \frac{1 - \sin^2 \theta}{\cos^2 \nu}$$

The program calculates $\sin^2(\tau/2)$ and selects the corresponding value of A^* by linear interpolation. In the case of spherical crystals, again $\nu = 0$ so that $\sin^2(\tau/2) = \sin^2\theta$.

Absorption correction decks are prepared by reading values of A^* from plots of A^* vs. $\sin^2\theta$, at .01 increments of $\sin^2\theta$, between 0.00 and 1.00. A new plot is required for each value of μR . Some judgement must be exercised in choosing the scale of the absorption correction factors in order to obtain the desired number of significant figures in the output.

"Sharpening" of intensities is performed according to the

relation:

$$F_o^2 \text{ (sharp)} = \frac{F_o^2}{\left(\sum_i f_i / \sum_i Z_i\right)^2} \exp \pm B^1 \frac{(\sin\theta)^2}{\lambda^2}$$

where f_i is the scattering factor and Z_i , the atomic number of the i -th atom and $\pm B^1$ is the artificial temperature factor.

Since the scattering factors decrease as θ increases, both the ratio of sums and the exponential term in the above expression tend to increase the value of intensity at higher angles whenever the artificial temperature factor is positive. The negative temperature factor is often used to diminish the sharpening effect of the ratio of sums. If no other guide is available B^1 may be tentatively adjusted so that the condition

$$\sum_{S_o^{-.1}}^{S_o} \langle F^2 \text{ (sharp)} \rangle = .1 \sum_i Z_i^2$$

holds, where $S_o = \frac{\sin\theta_{\max}}{2}$.

Program listing (in FORTRANSIT language)

```

0 0 DIMENSION ABCO (101)
0 0 READ, SWC1, SWC2
0 0 IF (SWC1) 1, 2, 1
1 0 READ, ABCO
0 0 READ, CSNU, CNU, CONST
0 0 IF (SWC2) 2, 3, 2

```

```
2 0 READ, BOLSQ, SAN, ATK1,
0 1 ATK2, ATK3, ATK4, CONST
3 0 READ, IND, INSFP, ISST
0 1 H, ISCF1, ISCF2, ISCF3,
0 2 ISCF4
0 0 VINT = INSFP*1.E-7
0 0 CINT = VINT
0 0 SSTH = ISSTH*1.E-10
0 0 IF (SWC1) 4, 5, 4
4 0 ASSUP = 1.-((1.-SSTH)/
0 1 CSNU)
0 0 JSSUT = ASSUP*1.E2
0 0 VINT = (ABCO(JSSUT + 1)
0 1 -(ASSUP*1.E2 - JSSUT)*
0 2 (ABCO(JSSUT + 1) - ABCO(
0 3 JSSUT + 2))) * CNU * VINT
0 0 CINT = VINT
5 0 IF (SWC2) 7, 8, 7
7 0 SHFC = SAN/(ATK1*ISC
0 1 F1 + ATK2 * ISCF2 + ATK3
0 2 * ISCF3 + ATK4 * ISCF4)
0 0 CINT = SHFC * SHFC * EXPF
0 1 (BOLSQ * SSTH) * VINT
8 0 VINT = CONST * VINT
0 0 STFC = SQRTF(VINT)
```

```

0 0 CINT = CONST * CINT
0 0 INTM = CINT * 1.E2
0 0 INTP = INTM * 100000
0 0 ISFP = STFC * 1.E2
0 0 INSFP = INTP + ISFP
10 0 PUNCH, IND, INSFP, ISS
0 1 TH, ISCF1, ISCF2, ISCF
0 2 3, ISCF4
0 0 GO TO 3
0 0 END

```

Standard Deviations Program

Introduction

The STD program computes standard deviations of observed structure factors on the basis of uncorrected film data. The output is easily reproduced into the standard input format of the I.B.M. 704 Crystallographic Least Squares Program (Busing and Levy, 1959).

Description of input cards

Constant card

/ I_b (7) /

I_b is value of the median intensity of the best judged range. It often coincides with 16 times the lowest ob-

servable intensity.

Data cards

/ hhkkl_laaaa / I_o (7) /

I_o is the uncorrected value of the observed intensity, aaaa = anything. These cards have the same format as the INCOR-I (Zalkin and Jones, 1957) data input cards.

/ hhkkl_laaaa / I_c (7), F_o(2) / a'a' ... a' ⁸/₉ /

I_c is the corrected value of the observed intensity, F_o is the observed structure factor ($=\sqrt{I_c}$), 8 in col. 30 indicates I_o ≥ I_p, 9 indicates I_o < I_p. Both the INCOR-I and the ACS output cards have the proper input format. These two types of data cards must appear in pairs with matched indices and in the order given.

Operating instructions

Loading sequence

1. STD Program deck, 2. Control card, 3. Data cards

Console settings

Storage entry: 70 1952 9999 (00 0000 1999 if program deck is already loaded).

Programmed:	STOP	Display:	PROGRAM
Half cycle:	RUN	Overflow:	SENSE
Control:	RUN	Error:	STOP

Operation

Use FORTRANSIT OBJECT wiring panel.

A legitimate machine stop is probably due to mismatched indices in data cards.

Computation times are 1.0 sec. per reflection for $I_{O} \geq I_b$, 2.5 sec. per reflection for $I_{O} < I_b$.

Description of output cards

/ h h k k l l a a a a / F_O (2) / $\sigma(F_O)$ (3) /

$\sigma(F_O)$ is the standard deviation of the observed structure factor.

Discussion

This program was designed primarily for use in conjunction with the Crystallographic Least Squares Program by Busing and Levy which employs the $\sigma(F_O)$ values for regulating the contribution of each reflection in the expression

$$R = \sum \left[\frac{1}{\sigma(F_O)} (|F_O| - |F_C|) \right]^2.$$

R is the function minimized with respect to crystallographic parameters by the least squares refinement, F_O and F_C are the observed and calculated structure factors, respectively.

The standard deviation of the best judged intensities ($I_{O} \geq I_b$) was estimated at 10%, that of the poorest judged (lowest observable), at 80%. Accordingly, this function was

expressed by

$$\frac{\sigma(I_o)}{I_o} = \begin{cases} 0.1 & \text{for } I_o \geq I_b \\ 0.1 \left(\frac{I_b}{I_o}\right)^{3/4} & \text{for } I_o < I_b \end{cases}$$

It was learned that the experimental errors of the corrections applied to I_o to obtain $I_c (= F_o^2)$ are much smaller than the error inherent in the visual judgement of intensities and can therefore be neglected. On the basis of this information and a standard statistical relation, one can write

$$\frac{\sigma(F_o)}{F_o} \approx \frac{\sigma(F_o^2)}{F_o^2} = \frac{\sigma(I_c)}{I_c} \approx \frac{\sigma(I_o)}{I_o}$$

or

$$\sigma(F_o) = \begin{cases} .05 F_o & \text{for } I_o \geq I_b \\ .05 \left(\frac{I_b}{I_o}\right)^{3/4} \cdot F_o & \text{for } I_o < I_b \end{cases}$$

The calculation of $\sigma(F_o)$ is performed according to these relations.

Program listing

Following is a FORTRANSIT listing of all program steps, along with comments explaining each operation.

0 0	READ, INB	read I_b
1 0	READ, IND, INT	read uncorrected data
0 0	READ, JND, JNSF, JSSTH	read corrected data

```

0 0 IF (IND-JND) 2, 3, 2      test for properly matched
                              indices
2 0 STOP
3 0 LSF = JNSF * 1000000     isolate  $F_0$  ...
0 0 NSF = LSF / 1000000     then shift back
0 0 LOD = JSSTH * 1000000000 isolate breaking code ...
0 0 KOD = LOD / 1000000000  then shift back
0 0 IF (KOD-8) 4, 4, 5      branch on breaking code
4 0 NSD = NSF / 2           calculate std. dev. for
                               $I_0 \geq I_b$ 
0 0 GO TO 6
5 0 L = INT / 1000          float 1000  $I_b/I_0$ 
0 0 A = INB / L
0 0 NSD ((A**.75)*NSF)     calculate std. dev. for
                               $I_0 < I_b$ 
0 1 / 353                  353 1000 x 2
6 0 PUNCH, IND, NSF, NSD   punch indices,  $F_0$ ,  $\sigma(F_0)$ 
0 0 GO TO 1
0 0 END

```

**APPENDIX B: OBSERVED AND CALCULATED
STRUCTURE FACTORS**

HKO STRUCTURE FACTORS FOR BISMUTH MONOCHLORIDE

H	K	OBS	CALC	H	K	OBS	CALC	H	K	OBS	CALC	H	K	OBS	CALC
2	748	645-		318	278	239-		617	174	135		912	241	264-	
4	558	636-		4		728	610-	618	95	93-		914	430	402	
6	239	292		4	1	143	97	7	1	281	241-	915	84	115	
8	381	449-		4	2	402	370-	7	2	183	157-	916	106	23	
10	229	304-		4	3	612	565	7	3	865	924	917	112	104-	
12	180	250		4	4	453	385	7	4	690	678	10		455	403-
14	107	108		4	5	1091	113-	7	5	986	864-	10	1	163	143-
16	326	378-		4	6	171	136	7	6	513	424-	10	2	908	1047
18	253	258		4	7	562	518	7	7	254	182-	10	3	103	65-
1	3	336	422	4	8	300	286	7	9	603	572	10	4	331	286-
1	4	93	64	4	9	519	472	710		265	269-	10	5	197	140-
1	5	513	610	4	11	438	516-	711		409	402	10	6	175	158-
1	6	90	75-	4	12	126	115	712		104	126	10	7	166	140-
1	7	308	379-	4	13	188	242	713		222	260-	10	8	157	105
1	8	274	405	4	16	122	94-	714		218	148-	10	9	190	117-
1	9	124	62-	4	17	211	193-	715		90	52-	10	10	333	260-
1	10	112	155-	4	18	95	110	716		131	136	10	11	155	71
1	11	495	681-	4	19	136	128-	717		129	118	10	16	79	100
1	12	96	75	5	1	108	88	718		144	91	10	17	102	119
1	13	231	248	5	2	142	124-	8		678	744-	11	1	482	526
1	16	253	245-	5	3	748	749-	8	1	118	99-	11	2	859	1004-
1	17	142	136	5	5	181	130-	8	3	147	97	11	3	102	77-
2	2	280	272	5	6	103	68	8	4	171	142	11	4	313	272
2	4	467	536	5	7	427	365	8	5	205	146-	11	6	428	308
2	5	620	736	5	9	337	330	8	6	489	378	11	7	265	228
2	6	890	1206-	5	10	222	253-	8	7	175	92	11	8	734	656-
2	7	154	117	5	11	188	173	8	8	270	281-	11	9	902	880-
2	8	176	224	5	12	468	487	8	9	405	320-	11	10	243	297
2	9	272	283-	5	13	176	146	8	11	95	79-	11	11	152	138
2	10	407	477	5	14	240	275-	8	14	151	106-	11	12	259	251
2	11	494	603	5	15	171	154-	8	15	71	49-	11	13	91	88-
2	12	220	278-	5	17	197	140-	8	16	350	294	11	14	231	268-
2	15	360	391-	5	18	47	78	8	17	259	275	11	15	149	143
2	17	110	96	5	19	82	100	8	18	82	89-	11	16	164	83
2	19	144	174-	6		514	404-	9	1	509	544	11	17	40	3
3	2	133	122-	6	1	823	864-	9	2	664	663	12		204	217
3	3	567	557-	6	2	528	547-	9	3	163	144-	12	1	124	114
3	4	261	260	6	3	525	489	9	4	321	280-	12	2	558	617
3	5	799	872	6	4	240	208	9	5	409	351-	12	3	101	17
3	6	348	391-	6	5	243	126	9	6	685	613-	12	4	268	290-
3	7	162	192-	6	6	872	837	9	7	307	270	12	5	189	84-
3	8	601	759	6	8	151	136	9	8	654	584	12	6	86	54-
3	9	281	269	6	10	252	213-	9	9	335	286-	12	8	277	173-
3	10	86	65	6	11	108	108-	9	10	432	395-	12	9	293	216
3	16	77	52-	6	14	241	250	9	11	171	167	12	10	133	47

H	K	OBS	CALC	H	K	OBS	CALC	H	K	OBS	CALC	H	K	OBS	CALC
1211	101	18-		1515	163	148-		19	7	161	119-	2310	65	48	
1212	74	61		1516	87	75-		19	8	221	225-	2311	104	82-	
1213	141	170		16	459	450-		19	9	86	120	2312	91	56-	
1214	299	254-		16	1	238	245	1911	72	93		24	1	250	266
1216	60	70		16	2	85	57-	1913	74	17		24	3	225	207
1217	252	248-		16	3	261	268-	1914	80	47		24	4	145	118
13	1	507	583-	16	5	426	391	20		646	737	24	5	361	334-
13	2	263	238	16	6	166	117	20	2	259	263-	24	6	189	133-
13	3	1110	1180	16	7	105	37	20	3	170	199-	24	7	291	228
13	4	486	475-	16	8	189	187	20	4	89	75-	24	8	104	109
13	5	218	177-	16	9	270	270-	20	6	241	244	24	9	148	84
13	6	511	408	16	10	239	199	20	8	177	147-	24	10	60	35-
13	8	286	284	16	11	166	198	20	10	244	240-	24	11	86	90-
1312	124	81-		16	12	113	110	20	11	236	137-	25	2	183	188-
1313	319	289-		16	14	80	32-	20	12	90	110	25	3	111	83-
1315	240	232		16	15	144	129-	20	14	156	178	25	4	219	161
1316	92	105-		17	1	155	106-	21	1	77	114	25	5	161	183
1317	59	47		17	3	161	130-	21	3	174	193	25	6	150	85
14		189	224	17	4	127	140	21	4	129	108-	25	7	90	15
14	1	290	323	17	5	107	59	21	6	98	84-	25	8	110	113
14	3	100	71-	17	6	149	188	21	7	303	208-	25	9	110	80
14	4	440	435-	17	7	79	37-	21	8	119	82-	25	10	56	9-
14	5	311	307	17	8	494	458-	21	9	175	178	26		112	99
14	6	395	354	17	9	254	261	21	11	247	253-	26	1	251	239-
14	7	137	146-	17	10	228	138	21	12	144	107	26	2	200	168-
14	9	209	164	17	11	139	122	21	13	129	108	26	3	242	272
1410	90	91		17	13	130	98-	22		153	125	26	4	54	82-
1411	287	196		17	15	95	72	22	1	265	292-	26	5	222	192
1412	97	90		18		273	369-	22	3	185	166-	26	6	170	144
1413	266	171-		18	1	290	310	22	4	410	354	26	7	139	135-
1414	70	124-		18	3	95	120-	22	5	161	132	26	8	125	136
1416	88	32-		18	4	233	265	22	6	327	272-	26	9	60	14
1417	164	181-		18	5	81	127-	22	7	177	135-	27	1	168	162-
15	1	150	142-	18	6	247	244-	22	8	109	112-	27	2	94	31
15	2	200	190	18	8	114	111	22	9	90	114-	27	6	62	61
15	3	507	442-	18	9	153	144	22	10	194	168	28		135	106-
15	5	177	148	18	11	386	277-	22	11	290	258	28	1	84	57-
15	6	175	104	18	12	82	29-	22	12	148	158-	28	2	41	49-
15	7	721	674	18	13	102	129-	23	1	164	136	28	3	107	128
15	8	156	124	18	14	187	132	23	2	88	105-	28	4	40	46
15	9	242	250-	18	15	279	260	23	3	109	69-	28	5	39	54-
1510	259	225		19	1	157	201	23	5	261	242				
1512	327	304-		19	2	354	350	23	6	157	132-				
1513	280	234		19	3	140	128-	23	7	120	105-				
1514	160	147		19	4	196	162-	23	8	236	202				

HK1 STRUCTURE FACTORS FOR BISMUTH MONOCHLORIDE

H	K	OBS	CALC	H	K	OBS	CALC	H	K	OBS	CALC	H	K	OBS	CALC
	9	189	213		317	164	144		611	132	143-		911	163	131
	11	112	105-		318	123	91		612	240	259		912	256	187
	13	446	551		319	25	37		613	102	63-		914	151	97
	15	94	71		402	398	412		614	145	179-		917	60	20
	17	89	92-		404	208	194-		615	231	232-		1001	277	310
1	2	343	430-		405	275	290		617	52	37		1002	214	238-
1	3	443	536-		406	680	692-		618	54	53		1003	452	462-
1	6	96	36-		407	123	83-		700	290	296-		1006	206	176
1	8	158	197-		408	73	6-		702	135	134		1007	125	17
1	9	121	100-		409	166	159		703	675	711		1008	460	418
110	122	149			410	84	81-		704	324	271		1009	188	193-
111	195	272			411	165	179-		705	160	137		1010	97	99-
112	129	131			412	306	323		707	244	221		1011	361	405
113	96	138-			413	216	276-		708	176	157-		1012	222	184-
114	116	146			414	75	67		709	264	212-		1013	97	66
115	100	55-			415	92	109		710	185	207		1014	99	68-
117	179	211			417	117	102-		711	225	204-		1015	107	70
119	69	104-			418	129	123-		712	246	254-		1017	51	15
2	2	227	237-		500	341	326		713	121	132		1100	576	690-
2	3	210	227-		501	728	854-		714	124	128-		1102	211	200
2	5	126	151		502	148	32-		715	144	153-		1103	168	171
2	6	680	831-		503	125	35		716	156	150		1104	137	172-
2	7	184	218-		504	162	170-		717	44	15-		1105	89	29
2	8	269	306-		505	143	130		718	150	144-		1106	244	182-
2	9	93	104-		506	287	263		801	177	156-		1107	253	198-
210	205	184			507	130	118-		802	288	294-		1108	106	135
211	134	157			508	131	77		803	563	564		1109	110	32-
212	287	320			509	233	213		804	643	609		1110	102	148-
214	206	211			510	295	250-		805	493	483-		1111	195	179
215	102	34-			511	118	120-		806	244	212		1112	234	182
217	108	93			512	162	128-		807	155	159-		1113	200	140
218	39	32-			513	156	128-		808	491	444		1114	216	229
219	81	55-			514	157	190-		809	191	140		1115	116	119-
3	3	670	721-		515	114	104		811	153	95-		1117	129	93-
3	4	172	132		516	130	167-		812	377	341-		1201	196	156-
3	5	831	984-		517	118	84		813	125	93-		1202	241	298-
3	6	219	247-		518	83	59		814	166	129-		1204	245	257-
3	7	466	516		601	125	148		818	34	16-		1205	207	193-
3	8	277	294		602	125	102		901	422	469		1207	110	99-
3	9	138	110		604	84	55		903	692	715		1208	173	156-
311	203	220-			605	163	126		905	171	141		1209	204	183
312	108	59-			606	207	154		906	164	153		1210	160	149
313	136	155			607	387	367		908	323	223-		1211	178	150
315	101	38			609	241	226-		909	257	195-		1212	224	179
316	84	88-			610	300	290-		910	227	174-		1214	113	130-

HK2 STRUCTURE FACTORS FOR BISMUTH MONOCHLORIDE

H	K	OBS	CALC	H	K	OBS	CALC	H	K	OBS	CALC	H	K	OBS	CALC
2	774	739		4	2	302	336-	616	175	188		917	52	43	
6	483	553-		4	3	447	511-	617	66	73-		918	155	179	
8	337	448-		4	4	220	165-	618	207	199-		10	540	532	
10	404	504		4	5	685	682	7	1	336	359	10	2	251	251
12	135	126-		4	6	523	514	7	2	208	183	10	3	155	150-
14	286	403-		4	7	138	132-	7	3	733	755-	10	4	77	107
16	238	278		4	8	118	75	7	5	296	256-	10	5	211	188
18	39	65-		4	10	276	282-	7	7	458	410	10	6	564	470-
1	2	78	17-	4	11	303	297	7	8	570	599-	10	7	261	175-
1	3	288	246	4	12	205	236	7	10	197	155	10	9	213	148-
1	4	216	224-	4	13	180	123-	7	12	179	182-	10	10	239	207-
1	5	79	41-	4	15	111	130-	7	13	333	337	10	11	190	140
1	7	155	199	4	16	129	145-	7	14	84	96	10	12	175	115-
1	9	483	650-	4	17	130	145-	7	15	327	327-	10	13	108	101-
111	213	216-		4	18	87	100	7	16	116	130	10	14	150	110
114	171	153		5	1	509	529-	7	17	87	63-	10	16	69	104-
115	109	70		5	2	960	1134	7	18	68	58	10	17	78	64
116	157	143-		5	3	152	126-	8		453	413	11	1	98	120
118	38	55-		5	4	671	687-	8	1	537	557	11	2	169	135
2	1	646	807	5	5	273	258-	8	2	531	565-	11	4	421	392-
2	2	414	366	5	6	378	331	8	3	345	342-	11	5	436	401
2	4	565	611-	5	7	109	104-	8	4	78	94	11	6	159	113-
2	5	397	483-	5	8	145	139	8	5	371	306-	11	7	565	495-
2	6	78	81-	5	9	614	577	8	6	341	253	11	8	414	366
2	7	435	508	5	10	141	137-	8	7	145	104	11	9	215	161-
2	9	221	254	5	11	314	286	8	8	338	258-	11	10	109	15-
210	184	224-		5	13	215	188-	8	9	211	176-	11	11	196	161-
215	80	46		5	14	117	182	8	10	196	144-	11	12	210	155-
216	104	100-		5	15	104	69-	8	11	206	184-	11	13	111	104-
217	149	194-		5	16	119	115-	8	13	80	19	11	14	143	76
3	2	392	422-	5	17	68	47-	8	14	127	96	11	15	98	86
3	3	144	129	6		1190	1555-	8	15	132	121	11	16	86	52
3	4	442	421	6	1	80	153	8	17	104	100	11	17	82	74
3	5	79	49	6	2	259	261-	9	2	351	345-	12		545	658
3	6	325	312	6	3	299	257-	9	3	395	378	12	1	233	209-
3	8	287	282-	6	4	642	636	9	4	334	283	12	3	211	180
3	9	152	120-	6	5	336	256	9	6	76	84	12	4	128	149-
310	411	481		6	7	128	169-	9	7	647	564-	12	6	320	204-
311	191	159		6	8	216	176	9	8	604	516-	12	7	188	163-
313	187	238-		6	9	208	230	9	9	348	294	12	9	202	102
315	87	93		6	10	314	314	9	10	121	80	12	13	155	143
316	124	108-		6	11	144	92-	9	11	177	151-	12	14	77	73-
318	127	89-		6	12	216	214-	9	13	142	124-	12	15	70	33-
4		347	312-	6	13	195	209-	9	14	106	81	12	16	189	130-
4	1	210	198-	6	14	108	90	9	15	120	120	12	17	177	133-

H	K	OBS	CALC	H	K	OBS	CALC	H	K	OBS	CALC	H	K	OBS	CALC
13	2	222	211-	1609	82	44-		2005	269	265-		2603	96	137	
13	3	251	205-	1611	291	200-		2006	183	167-		2605	128	110	
13	4	230	272-	1612	166	137		2008	207	218-		2606	69	66-	
13	5	331	306	1613	56	69		2010	72	69		2607	104	127-	
13	6	299	237	1615	50	58-		2011	271	217-		2608	41	84	
13	7	267	197	1701	131	162-		2012	167	104-		2702	78	72	
13	8	306	255	1702	269	298		2013	107	89		2703	186	188-	
13	9	244	215-	1703	129	104-		2103	315	312		2704	38	36-	
1311	455	356-		1704	72	121		2105	338	330-		2706	164	181	
1312	164	161		1705	127	103-		2106	103	116-		2707	141	154	
1313	261	274		1706	289	262-		2108	125	74-		2800	100	99	
1314	160	171-		1708	339	280		2109	132	111-		2801	133	144	
1315	70	59-		1709	219	227		2111	106	95-		2802	141	148-	
1316	69	69-		1710	226	234-		2112	112	93		2901	77	90-	
14	1	186	186-	1711	153	128		2200	296	270					
14	2	135	119-	1713	99	111-		2201	110	76					
14	3	309	298	1715	72	87		2202	77	80					
14	4	165	149	1800	379	401-		2203	131	104-					
14	6	302	261-	1801	460	535-		2204	142	120-					
14	8	100	12-	1804	178	151-		2205	177	160-					
14	9	115	38	1805	287	248		2206	131	134					
1410	364	324		1806	141	119		2207	89	75					
1411	157	113		1807	160	170-		2208	188	167-					
1412	165	213-		1808	168	123		2210	143	119-					
1414	162	122-		1809	182	115-		2211	92	36					
1415	175	86-		1810	260	180-		2302	128	163-					
15	1	338	377-	1812	77	106		2304	90	101					
15	2	431	448-	1813	69	94-		2309	154	154-					
15	3	125	104	1814	89	98		2311	30	17					
15	4	458	440	1901	204	230		2312	9	25-					
15	6	72	34-	1902	117	131		2400	120	132-					
15	7	119	54	1903	227	259-		2402	130	125					
15	8	124	78	1905	112	116-		2403	63	41-					
15	9	120	64	1906	159	120-		2404	81	97-					
1510	156	125		1907	96	85		2405	128	120					
1514	165	160-		1908	159	158-		2410	51	66-					
1515	82	95-		1909	178	136-		2501	107	149-					
16	1	323	369	1910	110	175-		2502	77	60					
16	2	262	310-	1911	284	197		2504	77	101-					
16	3	310	292	1912	231	181		2505	100	96					
16	4	122	150-	1913	40	10		2506	156	111					
16	5	314	305-	1914	50	26-		2508	67	105					
16	6	347	317	2000	236	278-		2509	89	63					
16	7	473	410	2001	149	160-		2600	203	193-					
16	8	166	101	2002	205	227		2004	166	152					

HK3 STRUCTURE FACTORS FOR BISMUTH MONOCHLORIDE

H	K	OBS	CALC	H	K	OBS	CALC	H	K	OBS	CALC	H	K	OBS	CALC
	1	398	476-	3	8	386	320	6	17	108	115	9	15	144	176-
	3	1184	1239	3	10	234	216-	6	18	73	52-	9	16	37	28
	5	911	919-	3	11	89	105	7		801	853	9	17	72	72
	7	138	125-	3	12	101	164	7	1	800	835	10	1	88	100
	9	189	166	3	16	102	50-	7	2	309	311-	10	2	187	194-
	11	296	378	3	17	128	98	7	3	186	180	10	3	371	289-
	15	304	290	4	1	106	118-	7	5	268	218	10	4	198	155-
1	1	335	285	4	3	174	151	7	6	328	279	10	5	409	310
1	2	259	213	4	5	215	160	7	7	154	198	10	6	229	242
1	3	507	533-	4	6	88	58	7	8	180	91-	10	7	449	538-
1	4	322	290-	4	7	97	41	7	10	114	104-	10	8	244	229
1	5	265	222-	4	8	761	982-	7	11	216	219-	10	9	402	357
1	6	264	234	4	10	335	357	7	13	90	52-	10	10	109	20
1	7	115	116	4	11	79	3	7	14	86	86	10	11	209	192
1	8	282	245-	4	12	287	324	7	16	108	97-	10	12	223	205-
1	9	147	128	4	13	287	317-	7	17	218	185-	10	17	168	127
1	10	155	138	4	15	90	147	7	18	54	38-	11		223	220-
1	12	168	179	4	17	94	84-	8	1	127	118	11	1	396	392
1	13	230	218-	5		308	296-	8	2	266	249-	11	2	151	112-
1	15	166	139	5	2	292	304	8	4	526	513	11	3	324	332
1	16	236	232	5	3	509	481-	8	6	522	497	11	4	330	329
1	17	81	52	5	4	268	283	8	9	221	184	11	5	506	545-
1	18	71	108-	5	5	194	162	8	10	105	127	11	6	539	530-
2	1	412	356	5	6	202	182-	8	11	340	336-	11	8	195	173
2	2	517	489	5	7	156	177-	8	12	339	365-	11	9	181	196
2	3	570	527-	5	9	300	309	8	13	115	217	11	10	76	43
2	4	346	331-	5	10	136	128	8	14	84	86-	11	11	200	172-
2	5	170	108-	5	11	125	116-	8	15	77	64-	11	13	235	194
2	6	594	686-	5	12	266	265-	8	16	97	38-	11	14	297	306
2	7	440	534	5	13	189	195-	8	17	66	61-	11	15	77	63
2	9	528	626-	5	14	243	280-	9		179	144	11	16	60	29-
2	10	144	176	5	15	196	249	9	1	223	149	11	17	160	165-
2	11	279	338	5	16	78	38	9	2	133	143-	12	1	167	139
2	13	198	151	5	17	67	63-	9	3	254	232	12	2	211	190-
2	14	474	429	5	18	58	35	9	4	392	376	12	3	356	313-
2	16	130	105-	6	2	716	807	9	5	770	812	12	4	276	280-
2	17	58	45-	6	3	408	375	9	6	314	256-	12	5	84	128
2	18	141	123-	6	4	476	519-	9	7	372	300-	12	6	162	113-
3		595	482-	6	6	358	342	9	8	150	96-	12	8	89	75
3	2	476	460	6	7	149	121	9	9	415	413-	12	9	245	221
3	3	941	1176-	6	11	161	124-	9	10	88	84	12	10	153	69
3	4	463	429-	6	12	207	180-	9	11	398	475	12	11	171	126-
3	5	212	211-	6	13	151	176-	9	12	111	74	12	12	147	137
3	6	320	297	6	14	180	136	9	13	85	108-	12	13	257	233
3	7	169	175	6	15	157	152-	9	14	228	147	12	14	109	116-

H	K	OBS	CALC	H	K	OBS	CALC	H	K	OBS	CALC
1215		55	22	1610		148	110-	2104		79	70-
1216		127	141	1611		168	169-	2105		88	75-
13		748	912	1614		166	150	2106		201	207
13 1		558	648-	1700		293	298	2108		224	190-
13 2		547	598-	1701		127	88-	2109		112	108
13 3		153	128-	1702		105	74	2112		145	112
13 4		94	99-	1703		194	164	2201		114	114
13 5		72	74-	1704		178	169-	2202		104	43
13 6		375	340	1705		248	173-	2203		130	90-
13 7		328	316-	1706		179	141	2204		227	222-
1311		138	141	1707		297	263	2205		226	261-
1312		144	137	1708		133	56	2206		72	47-
1314		85	108	1709		72	8	2207		245	211
1316		137	139-	1710		282	204-	2208		185	216
14 1		254	245-	1711		176	212-	2211		138	125
14 2		202	184-	1714		103	100-	2300		293	336-
14 3		103	53	1801		261	245	2302		122	76
14 5		130	131	1802		150	142	2303		189	181-
14 6		297	293-	1803		101	155-	2304		86	58-
14 8		94	67-	1804		290	273	2306		88	97
14 9		191	173	1805		133	146	2308		78	91
1410		214	164-	1806		196	147	2309		171	114-
1411		124	155-	1809		331	313-	2402		299	344-
1412		282	342	1810		194	197-	2403		72	56-
1413		136	103	1812		119	136	2407		94	73
1415		111	134-	1813		46	20-	2408		211	243-
1416		58	31-	1814		112	113-	2500		212	229-
15		156	126-	1900		177	170-	2501		62	68
15 1		271	255-	1901		220	215-	2502		93	86
15 3		160	169-	1902		277	296	2503		103	132-
15 4		286	261	1903		284	285	2505		41	20-
15 5		261	240-	1904		96	57	2601		65	80-
15 6		262	258-	1905		209	242	2602		167	207
15 7		234	235	1906		107	109-	2603		142	102
15 8		207	122	2003		327	366	2604		283	262-
1510		309	305	2004		168	117	2605		64	64
1512		271	255-	2005		329	325-	2606		60	51
1514		174	146-	2006		78	100	2700		118	134
1515		73	62-	2008		123	98	2701		53	35
16 3		140	120	2009		82	81	2703		49	51-
16 4		294	277	2011		88	143	2704		77	78-
16 5		289	277	2013		55	49-	2705		87	73
16 6		410	507-	2100		113	121-	2801		45	28
16 8		156	124	2101		83	141	2803		49	33
16 9		76	1-	2103		152	134				

HK4 STRUCTURE FACTORS FOR BISMUTH MONOCHLORIDE

H	K	OBS	CALC	H	K	OBS	CALC	H	K	OBS	CALC	H	K	OBS	CALC
		1734	1956	3	9	141	167-	6	13	136	75-	10	6	509	563-
2		196	82	3	10	217	265	6	14	171	168	10	7	148	132-
4		467	437-	3	11	83	84	6	15	162	138	10	9	117	104-
6		109	83	3	12	63	57-	6	16	62	33	10	10	61	12
8		365	431-	3	16	117	86-	7	2	257	220	10	11	82	78
12		113	133	3	17	82	36-	7	3	251	209	10	12	125	185-
14		153	140-	4		781	697-	7	4	181	151	10	15	53	47
18		98	102	4	1	154	83	7	5	471	456-	10	16	76	86
1	2	414	354	4	2	158	123-	7	6	226	169-	11	1	374	354
1	3	565	562	4	4	301	239	7	8	184	183-	11	2	417	454-
1	4	289	307-	4	5	254	185-	7	9	338	371	11	3	153	120-
1	5	181	122	4	6	71	74	7	11	144	149	11	5	282	272
1	6	154	115-	4	7	179	159	7	12	117	126-	11	6	122	84
1	7	177	162-	4	8	153	183	7	15	147	125-	11	7	96	117-
1	8	391	482	4	9	213	219	7	16	96	105	11	8	234	211-
1	9	225	216-	4	11	128	107-	7	17	36	39	11	9	418	447-
1	10	65	100-	4	12	87	81	8	1	109	43-	11	10	137	162
1	11	266	326-	4	13	94	66	8	2	316	327-	11	11	82	33-
1	12	147	153-	4	16	42	23-	8	3	253	187-	11	12	62	72
1	13	67	39	4	17	175	178-	8	5	246	161	11	14	61	114-
1	14	189	222	5	1	276	240-	8	6	340	376	11	15	86	79
1	15	135	109	5	2	142	121	8	8	155	196-	11	16	121	79
1	16	162	184-	5	3	201	151-	8	9	323	332-	12		623	648
1	17	108	98	5	4	190	135-	8	10	120	79-	12	1	155	157
1	18	118	108-	5	5	159	162-	8	16	130	82	12	2	144	157
2	2	434	319	5	6	285	287	8	17	173	219	12	3	143	140
2	3	198	178-	5	8	168	207-	9	1	315	325	12	4	261	252-
2	4	149	65-	5	9	390	459	9	2	247	191	12	5	262	245-
2	5	346	324	5	11	239	226	9	4	106	72-	12	8	91	84-
2	6	451	461-	5	12	231	234	9	5	121	117-	12	9	308	234
2	7	158	158	5	13	100	84-	9	6	217	216-	12	10	115	106-
2	8	159	137	5	14	118	115-	9	7	97	57-	12	12	96	87
2	9	109	69-	5	15	101	60-	9	8	71	49	12	13	126	162
2	10	124	100	5	16	79	41-	9	9	63	18-	12	14	85	94-
2	11	263	352	5	17	58	47-	9	10	137	143-	12	15	39	53
2	12	86	78-	6		475	482-	9	12	126	142-	12	16	104	86-
2	15	198	192-	6	1	115	23	9	13	63	65	13	1	284	270-
2	16	62	28-	6	2	404	388-	9	14	213	250	13	3	496	529
3	1	295	213	6	3	137	91	9	15	86	69	13	4	217	223-
3	2	310	206-	6	4	193	219	10		272	263-	13	6	390	299
3	3	531	568-	6	6	480	468	10	1	74	13	13	7	92	51-
3	4	264	230	6	8	117	114	10	2	544	618	13	8	151	194
3	5	394	419	6	9	202	208	10	3	177	118-	13	9	86	26
3	7	271	250	6	10	95	55-	10	4	243	223	13	11	175	171-
3	8	169	151	6	11	199	221-	10	5	102	29-	13	12	81	78

H	K	OBS	CALC	H	K	OBS	CALC	H	K	OBS	CALC
1313		69	36-	1704		157	154	2204		82	98
1314		97	134-	1705		84	24	2205		68	23
1315		99	101	1706		83	63-	2206		47	58-
14		190	214	1707		104	112	2207		70	59-
14 1		153	185-	1708		113	81-	2208		102	115-
14 2		141	130-	1709		145	93	2209		70	42-
14 3		66	95	1711		73	96	2301		125	144
14 4		96	147-	1714		44	23	2302		175	152-
14 5		330	349	1800		234	268-	2303		114	108-
14 6		113	126	1801		72	42-	2304		110	51
14 7		146	171-	1806		62	7-	2305		113	129
1410		147	146	1808		152	105	2306		70	57-
1411		242	252	1810		133	98-	2307		94	72
1412		68	11-	1811		177	163-	2308		56	75
1413		91	71-	1901		91	116	2309		156	183-
1414		84	84-	1906		74	2-	2400		120	91-
1415		131	98-	1907		163	76-	2401		154	171
15 1		220	250-	1908		207	247-	2402		126	116
15 2		109	42	1909		78	50	2403		74	63
15 3		163	110-	1910		85	79-	2404		76	46
15 5		152	96	1911		167	152	2405		149	110-
15 6		66	55-	1912		163	140	2406		131	106-
15 7		291	285	2000		248	232	2407		150	122
15 8		302	248	2001		143	128-	2408		35	75
1510		131	77	2002		64	11-	2501		79	105-
1511		91	82	2005		142	89-	2502		58	106-
1512		190	156-	2006		128	99	2503		52	60
1513		98	84	2008		168	163-	2504		84	74
1514		67	50	2009		62	23	2505		89	108
1515		112	105-	2010		101	88-	2506		124	124
16		327	391-	2011		178	140-	2601		38	44-
16 1		242	234	2101		60	45	2602		59	91-
16 2		154	84-	2102		121	123	2603		133	181
16 3		91	39	2103		261	287	2604		80	69-
16 4		130	57	2104		158	167-	2605		78	105
16 7		217	201	2105		188	205-	2606		83	90
16 8		161	143	2106		201	146-	2701		67	90-
16 9		120	128-	2107		116	96-	2702		85	109
1610		181	190	2108		84	60	2703		37	43-
1611		64	11-	2110		87	70-				
1612		64	51	2111		113	125-				
1614		40	32-	2200		151	130				
17 1		74	8	2201		159	139-				
17 2		72	68	2202		120	95				
17 3		318	273-	2203		137	132-				

HK5 STRUCTURE FACTORS FOR BISMUTH MONOCHLORIDE

H	K	OBS	CALC	H	K	OBS	CALC	H	K	OBS	CALC	H	K	OBS	CALC
3	554	384-		3	8	106	153	6	7	290	305	9	13	99	11
5	121	33-		3	9	108	82	6	8	145	111	9	14	57	43
9	130	134		3	11	227	218-	6	9	262	218-	10	1	201	188
11	117	206-		3	12	64	80-	6	10	237	277-	10	2	102	118-
13	364	533		3	13	137	159	6	11	221	272	10	3	235	253-
15	88	34-		3	14	67	20	6	12	186	192-	10	4	70	55
17	94	102-		3	15	41	29	6	13	227	191-	10	5	225	180-
1	321	319		3	16	77	104-	7	1	522	483-	10	6	95	79
1 1	354	375-		3	17	105	106	7	2	193	121-	10	7	185	96
1 2	537	397-		4	1	122	84-	7	3	264	191	10	8	319	321
1 3	407	277-		4	2	406	340	7	4	545	539	10	9	232	245-
1 4	96	46		4	3	200	156-	7	5	234	233	10	10	79	103-
1 5	71	36-		4	4	181	184	7	6	171	154-	10	11	264	327
1 6	189	143-		4	5	525	586-	7	7	144	166	10	12	127	108-
1 7	134	37-		4	6	150	139-	7	8	168	164-	10	13	72	56-
1 8	95	109-		4	7	273	295	7	9	190	234	10	14	88	73
1 9	134	102-		4	8	123	139	7	10	122	152-	11	1	501	544-
110	106	129		4	9	220	188-	7	11	201	235-	11	2	158	152-
111	159	188		4	10	165	165-	7	12	127	148	11	3	207	192
112	51	55		4	11	187	197	7	13	158	155-	11	4	262	262-
113	46	41-		4	12	140	209-	7	14	177	149-	11	5	215	203
114	146	132		4	13	69	51	7	15	165	179	11	6	227	182-
115	108	64-		4	14	63	72	8	1	173	139-	11	7	61	83
117	146	174		4	15	56	17	8	2	310	241-	11	8	94	79-
2 1	136	78-		4	16	68	68-	8	3	468	473	11	9	132	155-
2 2	527	405-		5	1	375	279	8	4	445	441	11	10	212	219
2 3	110	73-		5	2	785	734-	8	5	451	419-	11	11	202	169
2 4	276	170		5	3	151	96-	8	6	120	107-	11	12	112	126
2 5	161	166		5	4	279	170	8	7	307	311	11	13	99	134-
2 6	523	513-		5	5	262	188-	8	8	200	177-	12	1	164	172-
2 7	326	337-		5	6	148	131	8	9	155	133-	12	2	120	143-
2 8	287	277-		5	7	262	243	8	10	125	117-	12	3	210	197-
2 9	157	69		5	8	136	105-	8	11	52	44	12	4	206	206-
210	208	132		5	9	87	60	8	12	63	52	12	5	171	132-
212	251	302		5	10	127	84	9	1	422	357	12	6	102	88
214	66	66		5	11	226	245-	9	2	104	83	12	7	89	99
215	57	30-		5	12	111	69-	9	3	455	534	12	8	196	172
217	89	97		5	13	110	112-	9	4	201	183-	12	9	143	117
3 1	209	103-		5	14	55	10	9	5	138	105-	12	10	72	73-
3 2	100	18-		5	15	144	160-	9	6	243	218	12	11	75	72-
3 3	332	274-		6	1	180	130	9	7	169	122	12	12	101	108
3 4	255	158		6	2	129	52-	9	8	232	184-	13	1	334	295-
3 5	722	761-		6	3	217	187-	9	9	108	57-	13	2	132	150-
3 6	294	241-		6	4	179	146	9	10	197	207-	13	3	90	39
3 7	396	384		6	5	174	85	9	11	210	152	13	4	317	296-

H	K	OBS	CALC	H	K	OBS	CALC	H	K	OBS	CALC
13	5	187	206-	17	7	63	25	23	1	91	122
13	7	203	229-	17	8	53	12	23	2	127	117-
13	9	188	191	17	10	50	49-	23	4	141	124
13	10	219	213	17	11	67	47	23	5	114	129-
13	11	58	25	17	12	29	3	23	6	94	79-
13	13	53	13-	17	13	178	154-	23	7	42	4
13	14	101	135-	18	2	357	467	23	8	74	81
13	15	119	132	18	4	180	134-	24	1	48	26-
14	1	85	98-	18	5	257	214	24	2	85	109-
14	2	261	230	18	6	216	176	24	3	157	177-
14	3	86	79-	18	7	240	234-	24	4	72	62-
14	4	349	373-	18	8	65	76	24	5	46	59
14	6	111	99-	18	10	120	73-	24	6	166	173-
14	7	242	320	18	11	51	37-	24	7	51	54-
14	8	184	171-	18	12	100	120-	25	1	144	137-
14	9	182	204-	19	1	147	162	25	2	74	75-
14	10	57	37	19	2	74	67	25	3	26	7-
14	11	48	59-	19	3	111	106	25	4	36	43-
14	13	84	76	19	4	114	108	25	5	64	50-
14	14	168	187	19	5	84	90				
15		263	273	19	6	231	205-				
15	1	261	227	19	9	140	127				
15	3	382	404-	19	11	121	132-				
15	4	183	167-	19	12	67	61-				
15	5	154	135-	20	1	167	156				
15	6	133	106	20	3	178	170-				
15	7	215	169	20	6	174	196				
15	12	121	89-	20	8	53	72-				
15	14	79	61-	20	10	110	107				
16	1	66	93-	20	11	108	101-				
16	2	121	127-	21		239	234				
16	3	139	146	21	2	308	284-				
16	4	299	337	21	3	81	62				
16	5	132	134-	21	4	84	73				
16	8	328	408-	21	5	138	103				
16	9	78	59-	21	7	54	50-				
16	10	156	163	21	8	174	151-				
16	11	177	149-	21	10	44	24				
16	12	62	49-	22	1	72	39-				
16	13	61	99-	22	2	179	158-				
17		151	111	22	5	130	133-				
17	1	89	82	22	7	146	147-				
17	3	202	213-	22	8	85	67				
17	5	280	323	22	9	196	211				
17	6	52	77-	23		179	194-				